NASA Contractor Report 185273

Lightweight Linear Alternators With and Without Capacitive Tuning

Janis M. Niedra
Sverdrup Technology, Inc.
Lewis Research Center Group
Brook Park, Ohio

June 1993

Prepared for
Lewis Research Center
Under Contract NAS3–25266

National Aeronautics and
Space Administration

LIGHTWEIGHT LINEAR ALTERNATORS WITH AND WITHOUT CAPACITIVE TUNING

Janis M. Niedra
Sverdrup Technology, Inc.
Lewis Research Center Group
Brook Park, Ohio

ABSTRACT

Permanent magnet excited linear alternators rated tens of kW and coupled to free-piston Stirling engines are presently viewed as promising candidates for long term generation of electric power in both space and terrestrial applications. Series capacitive cancellation of the internal inductive reactance of such alternators has been considered a viable way to both increase power extraction and to suppress unstable modes of the thermodynamic oscillation. Idealized toroidal and cylindrical alternator geometries are used here for a comparative study of the issues of specific mass and capacitive tuning, subject to stability criteria. The analysis shows that the stator mass of an alternator designed to be capacitively tuned is always greater than the minimum achievable stator mass of an alternator designed with no capacitors, assuming equal utilization of materials ratings and the same frequency and power to a resistive load. This conclusion is not substantially altered when the usually lesser masses of the magnets and of any capacitors are added. Within the reported stability requirements and under circumstances of normal materials ratings, this study finds no clear advantage to capacitive tuning. Comparative plots of the various constituent masses are presented versus the internal power factor taken as a design degree of freedom. The explicit formulas developed for stator core, coil, capacitor and magnet masses and for the degree of magnet utilization provide useful estimates of scaling effects.

Lightweight Linear Alternators With and Without Capacitive Tuning

Introduction

The steady state power output of any practical alternator is limited by the removal of heat due to electrical losses and by internal inductive reactance, even if more shaft power were available and other limits were not approached. In rotary machines ranging from laboratory size to large turbo and hydro alternators this so-called synchronous reactance may be about 0.5 to over 1 per unit.[1] Indeed, such a fractionally high reactive voltage drop is deemed not entirely bad because it can reduce risk of damage to the alternator in case of load fault currents.

However, in space power applications the need to reduce generating system mass, and perhaps also volume, without sacrifice of efficiency is an important consideration. Likewise important is the need to suppress alternator inductance dependent unstable modes of oscillation in the free-piston Stirling engines (FPSE) that are now serving as drivers for permanent magnet excited linear alternators. Hence, series capacitive cancellation of the inductive reactance of such thermodynamic oscillator driven alternators is thought to be a viable way to increase the specific power (ref. [9], p. 8-18) and also to control unstable modes (ref. [5], p. 79). Indeed, this approach has been implemented in recently tested FPSE-driven linear alternator-resistive load configurations. Alternator inductance thus becomes a sensitive parameter in tradeoffs involving alternator and tuning capacitor mass, degree of magnet utilization, efficiency, and power available to a load.

The purpose of this study is to provide an overview of these tradeoffs and an estimate of trends in a setting of realistic ratings, while avoiding engineering design details, excessive machine computation and possibly misleading attempts at precision. The core observation is that the simple circuit equation for a loaded and tuned alternator can be rewritten in terms of power and exciting magnet and capacitor masses, provided one accepts a simplifying assumption regarding capacitor mass. Basic magnetics laws are then applied in the usual way to a single slot, permanent magnet excited linear alternator to derive relations between masses, reactive voltage drops, magnetization conditions, rated volt-amperes and power. Efficacy of capacitive tuning may then be judged versus the added complexity from plots of stator, magnet and capacitor masses as free parameters (e.g. the internal power factor (IPF)) are varied within limits defined by stability and magnetization constraints.

Precise evaluation of the effects on efficiency is not attempted here, because normally in good high power designs one expects this to be a question of just one or two percentage points out of say 90. The idealized models used in this analysis are not capable of providing such fine resolution in efficiency. However, checks are made to ensure that gross geometrical distortions, e.g. extreme coil-to-core mass ratios, detrimental to efficiency are avoided.

FPSE-driven linear alternators rated tens of KW and excited by high energy product samarium-cobalt magnets are considered promising candidates for reliable and efficient long term generation of electric power in space.[2] Although parameter values for illustrative plots were chosen to reflect conditions representative of such a machine, it is felt that most of these values, as well as modeling assumptions, are not overly specialized so as to preclude useful general conclusions.

Magnet and Capacitor Mass Related to Equivalent Circuit Parameters.

Since a main objective of this study is to argue for trends in mass variation with little given, apart from gross ratings and type of excitation, the simple equivalent circuit shown in Fig. 1 is suitable. The alternator is represented by a voltage source V_{gen} in series with linear lumped elements. Magnet parameters are at the heart of V_{gen} and the series inductance L_s. Hence, these related quantities need to be studied in some detail. Electrical losses are represented by a series resistance R_s. However, in a well designed machine these losses are small compared to the kVA rating and moreover, efficiency and its variation is not the prime issue here. Hence, R_s will simply be ignored by lumping it with the load. At the terminals of the machine the circuit is completed through a tuning capacitor C in series with a resistive load R_l. This tuning is allowed to be partial in the sense that the IPF $\equiv \cos \angle(\tilde{V}_{gen}, \tilde{I}) \leq 1$, including the case of no capacitor (i.e. $C \to \infty$); that is, here "tuning" does not imply resonance. This lets one explore fully the new degree of freedom introduced by a series capacitor.

Both the exciting magnet mass M_m and the tuning capacitor mass M_c can be related to the electrical quantities of Fig. 1, and hence to each other by the circuit equation. The form and basis of these relations will now be indicated, with details of the derivation of M_m from machine parameters given in Appendix A.

The smallest possible capacitor mass is assumed to be proportional to the reactive power P_c according to

$$M_c = K_c P_c = K_c I^2 / (\omega C), \tag{1}$$

where $\omega=2\pi f$ is the angular frequency and K_c is a constant. An analysis[3] of the ratings of several commercial ac power capacitors indicated that Eq. 1 is at least a fair approximation over a limited frequency range. A $K_c=3\times10^{-4}$ $kgV^{-1}A^{-1}$ appears conservative, whereas half of this would be beyond today's commercial technology.

M_m is involved through an equation relating the voltage drop $V_{Ls}=\omega L_s I$, the open circuit terminal voltage V_{gen}, the maximum volt-ampere rating P_{gen} of the machine, the ratio ℓ of slot leakage voltage to V_{gen}, the ratio K_1 of gap leakage to magnet reaction inductances, and a constant K_m whose reciprocal measures the magnet energy product per unit mass times the frequency and a gap factor:

$$\beta \equiv V_{Ls}/V_{gen} = [(1 + K_1) K_m P_{gen} / M_m] + \ell. \tag{2}$$

Eq. 2 is obtained from Eqs. A20, A21 and A23, and is based on a linearized magnetic circuit with geometrized leakage paths. The linearity assumption is quite good for intrinsically square loop magnets, such as the Sm_2Co_{17} type, in their normal region of use. Indeed, on the recoil line their permeability is only 3 or so percent above that of free space, making the body of the magnet act in effect like a large air gap in a circuit of magnetically soft material assumed not to be driven into saturation. Hidden in Eq. 2 is also the assumption that variations in magnet size are effected by uniform rescaling of all of the magnet's and the gap's dimensions. This conveniently preserves magnet shape and hence certain flux leakage ratios, but is felt not to be destructive to subsequent arguments. Questions of magnet, pole shoe and gap shape belong to machine design optimization studies[4], whereas here we are using idealized geometry for a comparative study of variations in magnet size to meet power factor, tuning or other conditions. Although magnet shape is included as an adjustable parameter, there seems no reason to expect that deviation from its normal optimum for a given magnet material and stator configuration would pay significant dividends.

Relation Between Magnet and Capacitor Masses

It remains here to relate M_m and M_c with the help of the circuital equation

$$I^2 R_\ell^2 + I^2 \left(\omega L_s - \frac{1}{\omega C}\right)^2 = V_{gen}^2 \tag{3}$$

written from Fig.1; note that the small R_s has not been distinguished from the load. The alternator is assumed to be delivering the maximum or rated power P_r at rated current I_r. But as one might expect, the alternator's mass has explicit dependence only on P_r, allowing some freedom in I_r, the load R_ℓ, the internal V_{gen}, and the IPF. Except for the IPF, which will serve as a free parameter, these degrees of freedom are, however, inessential to the analysis as long as Eq. 3 is satisfied.

Eq. 3 can be rewritten in the form

$$\alpha^2 + \left(\frac{V_{Ls}}{V_{gen}} - \frac{P_c}{P_{gen}}\right)^2 = 1, \tag{4}$$

where $\alpha \equiv IPF = IR_\ell/V_{gen}$. Substitutions from Eqs. 1 and 2 then produce the relation sought between M_m and M_c. However, for calculations involving these masses it is convenient to solve this relation for say M_c explicitly and also define new symbols for recurrent groups of geometric and electrical quantities. Hence, three new symbols are defined as follows:

$$M_{mo} \equiv \left[(1 + K_1)\, K_c\, K_m\right]^{1/2} P_{gen}, \tag{5}$$

$$\gamma_\pm \equiv \left(\ell \pm \sqrt{1 - \alpha^2}\right) \left[\frac{K_c}{(1 + K_1)\, K_m}\right]^{1/2}. \tag{6}$$

The contents of Eq. 4, when expressed in terms of M_c and M_m, then amounts to the two equations

$$M_{c\pm} = \left(\frac{M_{mo}}{M_m} + \gamma_{\pm}\right) M_{mo}, \tag{7}$$

where the "+" case corresponds to $1/(\omega C) > \omega L_s$ or equivalently to $\tilde{I}$ leading $\tilde{V}_{gen}$, and the "−" case to $\tilde{I}$ lagging $\tilde{V}_{gen}$. Thus when C is sufficiently large to make inductive effects predominate, the capacitor mass is given by M_{c-}.

M_c may decrease and approach zero, but clearly can not become negative. The "−" case of Eq. 7 covers the contents of this observation in the inequality

$$\left(\frac{M_{mo}}{M_m} + \gamma_{-}\right) \geq 0, \tag{8}$$

which when written out becomes

$$\frac{P_{gen}}{M_m} \geq \frac{(\sqrt{1 - a^2} - \ell)}{(1 + K_1)\ K_m}\ . \tag{9}$$

The special case of equality in Eq. 9 is important in its own right because it corresponds to no capacitor (nc). Hence it is repeated below for emphasis:

$$\left(\frac{M_m}{P_{gen}}\right)_{nc} = \frac{(1 + K_1)\ K_m}{(\sqrt{1 - a^2} - \ell)}\ . \tag{10}$$

Qualitatively Eq. 10 states what one might expect: even if coil leakage inductance were zero (ℓ=0), one needs a large magnet to achieve an IPF close to unity.

Approach to Evaluation of Capacitive Tuning Defined

In systems composed of diverse components often hard to quantify factors, such as overall reliability, weigh heavily in final design. For multiyear space missions, high alternator reliability must be achieved in a system requiring low mass and possibly low volume. Alternator reliability is sensitive to electrical insulation degradation due to the effects of temperature, radiation and corona, and hence is likely to improve rapidly with advances in technology. However, the mass of electromagnetic energy converters is tied to material properties and magnetics principles less subject to rapid evolution. Therefore, we choose to first compare the tuned and no-capacitor cases on the basis of mass, and look for significant differences to justify the use of capacitors.

The above mentioned principles and properties fix rather hard lower bounds to stator, magnet and capacitor mass, which can be incorporated using simple models. If a mass advantage deriving from these basics exists in one case or the other, then it must appear in any model faithful to these principles, even

if it be simple and geometrized. Otherwise, the existence of such a mass difference would rest on circumstantial complexities and would be of lesser interest here.

Appendix B shows by two such geometrized models incorporating limits on flux and current densities that the mass M_s of stator core plus copper coil varies as the product of a fractional power of the terminal volt-amperes P_t and an algebraic function of a length ratio s; both fractional power and algebraic function are geometry dependent. Moreover, at constant P_t the ratio s is adjustable to minimize M_s. As tuning conditions (IPF) and magnet or capacitor mass are varied within the constraint of Eq. 7, the shape factor s will generally deviate from the value s_o which minimizes M_s at constant P_t. Indeed, this may induce a significant deviation in M_s as the full range of the IPF is explored. The varied tuning conditions may also have a significant effect on the terminal voltage V_t, and hence on M_s through P_t. A detailed exposition of these dependences is given in the next section.

The models presented are thought to give the form of the dependence of M_s on P_t and on s to sufficient accuracy for a comparative study. To get realistic masses would require an increase in M_s by some practicability weighting factor, and also would require mass allowances for capacitor associated hardware, magnet transport cage or plunger, and so on. For comparison purposes, however, such weightings will be assumed to play no decisive role.

Stator Mass Related to Internal Power Factor and Magnet Mass

A. Parametrization of the stator mass.

Expressions (B14) and (B14') for the mass M_s of a bare stator consisting of a magnetic core and a coil are derived for the geometrized configurations of interlocked toroids and a long tube, respectively. They have the general form

$$M_s = P_t^r F(s), \tag{11}$$

where $0<r<1$, and the function F has a minimum at some value s_o of its argument. r, F and s_o are geometry dependent.

An important point about stator mass and capacitive tuning follows from Eq. 11 and will be discussed in the section "Comparative Analysis of Stator Mass". However, in order to make a quantitative assessment of the sensitivity to parameter variation it is necessary to derive additional equations that express the masses as functions of the degrees of freedom. α is chosen as the main free parameter of variation. Choice of the magnet mass M_m as some function of α gives an additional degree of freedom only in the tuned case. The development of the necessary equations now follows.

B. Terminal volt-amperes.

Considering the external circuit, the definition of α and Eq. 1, the terminal voltage is

$$V_t = \left[(\alpha\ V_{gen})^2 + \left(\frac{I}{w\ C}\right)^2\right]^{1/2}$$

$$= V_{gen}\left[\alpha^2 + \left(\frac{M_c}{K_c\ P_{gen}}\right)^2\right]^{1/2}, \qquad (12)$$

or equivalently,

$$P_t = P_{gen}\left[\alpha^2 + \left(\frac{M_c}{K_c\ P_{gen}}\right)^2\right]^{1/2}$$

$$= P_r\left[1 + \left(\frac{M_c}{K_c\ P_r}\right)^2\right]^{1/2} \qquad (13)$$

in terms of volt-ampere products. This can also be deduced from the vector diagram in Fig. 2. Note that P_r is always the real power, whether the alternator is tuned ($M_c>0$) or not tuned ($M_c=0$). Eq. 7 can be used to eliminate M_c from Eq. 13, which transforms the above P_t to the form desired for use in Eq. 11.

C. Shape scaling functions.

The shape factor s can likewise be expressed as an algebraic function involving w, P_r, other parameters and materials ratings, and the degrees of freedom, although now one is forced to specific geometries.

For the toroidal geometry the ratio V_t/V_{gen} is determined by Eqs. B5, A14, A8 and setting $x_o=w/2$:

$$V_t/V_{gen} = \pi\ (1 + K)\ B_s\ r_2^2/(A_m\ B_r). \qquad (14)$$

Using Eq. B11 to eliminate r_2 and Eq. 12 to eliminate V_t from Eq. 14 gives

$$(1 + K)\ B_s\ (A_p\ P_t)^{1/2}\ s = A_m\ B_r\left[\alpha^2 + \left(\frac{M_c}{K_c\ P_{gen}}\right)^2\right]^{1/2}. \qquad (15)$$

Finally P_t and A_p are eliminated by Eq. 13 and Eq. B8, respectively, and the result conveniently expressed as a formula for s^2 :

$$s^2 = \frac{w\ J_r\ (A_m\ B_r)^2\ \alpha\ D}{\sqrt{2}\ K_w\ (1 + K)^2\ B_s\ P_r} \quad , \tag{16}$$

where

$$D \equiv P_t/P_{gen} = \alpha\left[1 + \left(\frac{M_c}{K_c\ P_r}\right)^2\right]^{1/2} \quad . \tag{17}$$

The analogous result in the cylindrical case is

$$(s - 1)^2 = \frac{\pi\ w\ J_r\ (A_m\ B_r)^3\ D^2\ \alpha}{\sqrt{2}\ K_w\ (1 + K)^3\ B_s^2\ L^2\ P_r} \quad . \tag{18}$$

In these formulas for s the total cross-section A_m of magnets of any one orientation (see Fig. A1) is related to their volume $\mathcal{V}_m$ only by the stated convention that magnet shape shall be entered as an adjustable constant independent of other degrees of freedom. Accordingly in the toroidal case one can assume circular magnets of radius

$$r_m = (A_m/\pi)^{1/2} \tag{19}$$

and specify their height to be

$$h_m = 2\ a_h\ r_m \quad , \tag{20}$$

where a_h is the above mentioned constant. Introduction of the total magnet mass M_m and its density ρ_m, along with Eqs. 19 and 20, gives

$$A_m = \pi^{1/3}\left(\frac{M_m}{4\ \rho_m\ a_h}\right)^{2/3} \quad . \tag{21}$$

In the cylindrical case the length L does not scale, and a_h assumes the meaning of a magnet height-to-width ratio. For this case

$$A_m = \left(\frac{L\ M_m}{2\ \rho_m\ a_h}\right)^{1/2} \quad . \tag{22}$$

These formulas for A_m assume a single pair of oppositely oriented neighboring magnets and consequently $M_m = 2\rho_m \mathcal{V}_m$ from the definitions. The usual practical configuration of two pairs, which will be used later for making plots, is covered by the transformation $a_h \to 2a_h$ (see also Appendix A) with the above definitions of M_m and A_m maintained.

In the case of no capacitors, the magnet mass is given by Eq. 10. Using Eq. 10 along with Eq. 21, Eq. 16 for the toroidal geometry can be rewritten as

$$s^2 = \frac{\pi^{2/3}\, J_r\, [\mu_m\, (1 + K_1)]^{4/3}\, P_r^{1/3}}{\sqrt{2}\, a_h^{4/3}\, \omega^{1/3}\, K_w\, (1 + K)^{2/3}\, B_s\, B_r^{2/3}} \cdot \frac{\alpha^{2/3}}{(\sqrt{1 - \alpha^2} - \ell)^{4/3}} \,. \tag{23}$$

Similarly, Eq 18 for the cylindrical geometry can be rewritten as

$$(s - 1)^2 = \frac{2\, \pi\, J_r\, [\mu_m\, (1 + K_1)]^{3/2}\, (P_r/L)^{1/2}}{a_h^{3/2}\, \omega^{1/2}\, K_w\, (1 + K)^{3/2}\, B_s^2} \cdot \left(\frac{\alpha}{\sqrt{1 - \alpha^2} - \ell}\right)^{3/2} \,, \tag{24}$$

using Eqs. 10 and 22.

In the tuned case there exists the additional degree of freedom to trade off M_m versus M_c, subject to the restriction imposed by Eq. 7. Mathematically, this freedom means that one may choose M_m to be any physically acceptable function of α and then find M_c from Eq. 7 along the inductive and capacitive branches. However, as will be discussed, the particular choice $M_m = M_{mo}$ is privileged in that it minimizes $(M_c + M_m)$. For this reason it may be helpful to write M_m in the form

$$M_m(\alpha) = R(\alpha)\, M_{mo}(\alpha), \tag{25}$$

where R is any acceptable function of α or just a constant. $D_\pm$ is then determined for the two branches by the defining Eq. 17 and Eq. 7:

$$D_\pm^2 = \alpha^2 + (R^{-1} + \gamma_\pm)^2\, (1 + K_1)\, K_m / K_c. \tag{26}$$

Returning to Eqs. 16, 18, 21 and 22, the shape factors for the tuned case are thus found to be

$$s_\pm^2 = \frac{(\omega\, P_r)^{1/3}\, J_r\, [\pi\, B_r\, \mu_m\, (1 + K_1)\, K_c]^{2/3}}{2^{11/6}\, K_w\, B_s\, \rho_m^{2/3}\, [a_h\, (1 + K)]^{4/3}}\, \alpha^{-1/3}\, R^{4/3}\, D_\pm \tag{27}$$

and

$$(s_\pm - 1)^2 = \frac{\pi\, J_r\, \omega^{1/4}\, B_r^{3/2}\, [\mu_m\, (1 + K_1)\, K_c]^{3/4}\, (P_r/L)^{1/2}}{\sqrt{2}\, K_w\, a_h^{3/2}\, B_s^2\, \rho_m^{3/4}\, (1 + K)^{9/4}}\, \alpha^{-1/2}\, R^{3/2}\, D_\pm^2 \tag{28}$$

for the toroidal and cylindrical geometries, respectively. Along the inductive branch the domain of α is restricted such that

$$R^{-1} + \gamma_- \geq 0 \,, \tag{29}$$

which is merely a restatement of Eq. 8. At the point of equality (i.e. $M_c = 0$) in Eq. 29 the inductive branch of the tuned M_s versus α curve intercepts the no-capacitor M_s curve.

Comparative Analysis of Stator Mass

The stator mass of the models considered was found to be expressible in the form of Eq. 11, where the function F has implicit dependence on the ratings and parameters that determine power handling capacity, but has no direct dependence on α or other degrees of freedom. These degrees of freedom enter through the argument s of F, as was shown in the above section. It will now be shown that the minimum achievable stator mass of a machine designed not to be tuned is indeed the lowest possible stator mass. That is, a tuned design can not be below it.

To prove this, first observe that the minimum stator mass in a design using no capacitors (nc) is

$$(M_s)_{nc,min} = P_r^r \, F(s_o) \ , \tag{30}$$

where s_o is the point of minimum F(s), and the load power P_r appears because $P_t=P_r$ for a resistive load in the nc case. Moreover, this minimum is attainable because corresponding to s_o an acceptable α_o always exists to satisfy Eq. 23 or 24. The stator mass of a tuned (c) design can be written in the form

$$(M_s)_c = (P_t/P_r)^r \, P_r^r \, F(s) \ . \tag{31}$$

Since this F is the same as in the nc case, it follows that

$$P_r^r \, F(s) \geq P_r^r \, F(s_o) = (M_s)_{nc,min} \ . \tag{32}$$

As long as $M_c \neq 0$, Eq. 13 implies

$$P_t > P_r \ , \tag{33}$$

and hence that

$$(P_t/P_r)^r > 1 \ , \tag{34}$$

since r is positive. The conclusion

$$(M_s)_c > (M_s)_{nc,min} \tag{35}$$

now follows from Eqs. 31, 32 and 34.

Indeed, the argument leading to Eq. 35 is unaffected by the choice of the magnet mass in the tuned case because $R(\alpha)$ never enters into the argument. Different magnet shapes a_h may be chosen in the tuned and no-capacitor cases and still conclude the same thing. This is so because these degrees of freedom enter only through s, but have no effect on F itself. However, variation of these degrees of freedom alters the shape of $M_s(\alpha)$ plots and shifts the points where mass minimum is attained and where the tuned and no-capacitor curves merge. Illustrations of these behaviors are given in Figs. 3A and 3B which compare specific stator mass of the no-capacitor design as a function of α to that of tuned designs, using representative values of parameters and ratings, with $\ell=0$. For simplicity the R in Eq. 25 has been assigned various constant

values, and hence as $M_{c-} \to 0$ the inductive (lower) branches of the tuned curves terminate on the no-capacitor curve at various corresponding values of α (cf. comment after Eq. 29). But regardless of R, no tuned curve can ever dip below the minimum of the no-capacitor curve.

At the next level of sophistication, for each α one can ask for that value of R which minimizes either M_s, or even the total mass $M \equiv M_s + M_m + M_c$. Such a computation determining the function $R(\alpha)$, and thereby $M_m(\alpha)$, which for each α minimizes say M is numerically, although not algebraically, feasible. However, the conclusion given by Eq. 35 remains of course the same. Presentation of the results is deferred until after analysis of the magnet and capacitor masses.

Comparative Analysis of Magnet and Capacitor Mass

For the case of no tuning the specific magnet mass can be plotted from

$$\left(\frac{M_m}{P_r}\right)_{nc} = \frac{(1 + K_1)\ K_m}{\alpha(\sqrt{1 - \alpha^2} - \ell)} , \tag{36}$$

which is a trivial modification of Eq. 10. In the tuned case we consider the sum of magnet and capacitor masses, writing it in the specific form

$$(M_m + M_{c\pm})\ /\ P_r = \left(\frac{M_m}{M_{mo}} + \frac{M_{mo}}{M_m} + \gamma_\pm\right) M_{mo}/P_r \tag{37}$$

derived from Eq. 7, where

$$M_{mo}/P_r = [(1 + K_1)\ K_c\ K_m]^{1/2}\ /\ \alpha\ . \tag{38}$$

The LHS of Eq. 37 has a minimum at $M_m = M_{mo}$ with respect to variations in M_m. For $M_m < M_{mo}$ it rises rapidly as $M_m \to 0$, while for increasing M_m the rise is asymptotically linear except that in case of negative $\gamma_-(\alpha)$ the M_m is bounded from above in order to satisfy Eq. 8. It may be well to recall again that the choice of $M_m = M_{mo}$ does not generally minimize the M_s, although the difference may sometimes be negligible, as illustrated in Fig. 3.

Fig. 4 shows plots comparing specific magnet mass in the no-capacitor case with the minimized (Fig. 4A) and off-minimum (Fig. 4B) specific magnet plus capacitor mass in the tuned case for the range of α shown. Again representative values were chosen for the ratings and parameters, and the coil leakage ℓ has been neglected. In each figure, three tuned curves have been drawn, corresponding to K_c ranging from currently available values down to half of those values. The value of the free space gap fringing flux ratio K_ℓ chosen, based on taking $a_h = 1/3$ in the cylindrical geometry, is likely closer to reality than the high flux leakage of a disk-shaped gap in the toroidal geometry. In any case, if K_ℓ is increased then all curves are raised and the minimum at $\alpha = 1/\sqrt{2}$ in the no-capacitor curve sharpens. Deviation of M_m from M_{mo} also tends to raise the tuned curves, as is already known and illustrated in Fig. 4B.

Although there is an apparent similarity to the analogous stator mass curves, Fig. 4A shows that the magnet plus capacitor mass can dip slightly below the minimum of the magnet mass for no tuning. The relative mass reduction afforded by tuning is not impressive, unless for reasons such as engine stability or limits on the allowed demagnetizing B-field swing ΔB it is necessary to operate at an α close to unity in the no-capacitor case. A decrease in K_c likewise produces unimpressive improvement within this $M_m=M_{mo}$ scheme, and is finally limited by the allowed ΔB because Eq. 5 then forces the M_m to decrease also and hence the ΔB to increase. Moreover, at the power levels considered here, these magnet and capacitor mass reductions tend to be overshadowed by the considerably larger stator mass. Therefore even in the total mass minimizing scheme to be discussed next, as much as a twofold reduction in K_c would still give only a relatively minor reduction in M.

Minimum Total Mass – Results and Discussion

It is straight forward to find numerically, at each value of α, that value of the magnet mass M_m which minimizes the total mass $(M_s+M_m+M_c)$ in the tuned case. This procedure thus determines the function $R(\alpha)$, as defined by Eq. 25, giving a result different from the constant R=1 that was shown to minimize (M_m+M_c). The corresponding capacitor mass $M_c(\alpha)$ is then given by Eq. 7.

Such a computation was programmed for the toroidal geometry, using the mass formulas developed for M_s, M_m and M_c, and the results are presented in Fig. 5. The total specific mass, Fig. 5A, in the mass-minimized tuned case, has, as expected, a behavior similar to that of the stator mass for various fixed R plotted in Fig. 3A. The lower tuned curve in Fig. 5A starts at some point left of the minimum on the no-capacitor curve and dips, as α increases, slightly below that minimum before rising again to the point at resonance. The upper, or capacitive, branch then rises monotonically as α decreases. This dip is obviously minuscule and no significant mass reduction can be had by tuning, provided one may design for operation at an α near the minimum on the no-capacitor curve. Indeed, here a tuned design can have little mass advantage unless the no-capacitor α needs to be above say 0.95. The corresponding magnet and capacitor specific masses are shown in Figs. 5B and 5C, respectively.

Additional computations have shown that it is difficult to produce a significant dip in the tuned inductive branch within reasonable variations of the parameters. High magnetic fringing (a_h increased to 0.5), reduced capacitor specific mass ($K_c=1.5\times10^{-4}$), doubling of power to 50 kW, and reduction of B_s to 1 T had only a slight effect in this regard. The highest sensitivity was seen for a reduction of B_r to 0.7 T, but still the amount of dip was small. However, reduction of both B_s and B_r shifted the location of the no-capacitor minimum toward lower α and increased the rise of the no-capacitor curve above the tuned inductive branch. Hence if special circumstances, such as high temperature, greatly reduce B_s or B_r, and if stability requires a high no-capacitor α, then capacitive tuning might offer a mass savings. For example, the stability of free piston Stirling engines coupled to linear alternators has been reported to depend both on the ratio β (Eq. 2) as well as on the value of any series capacitance.[5] Maximum allowed values reported for β for various engines range from 3 for a tuned case down to 0.5 for a no-capacitor case. Since

$$\beta = \sqrt{1 - \alpha^2} \tag{39}$$

in the no-capacitor case (see Fig. 2), an α of 0.9 is then entirely sufficient to satisfy the lowest quoted upper limit on β. In Fig. 5A the minimum ordinate on the inductive branch of tuned designs is only about 3% below the no-capacitor mass at α=0.9. At this no-capacitor α and with B_r reduced to 0.7 T, but other parameters the same as in Fig. 5, the numerical studies show that the mass reduction gained by tuning increases to 11%. If in addition the B_s is reduced to 1 T, then one gets 16 %, as shown in Fig. 6. Moreover, from the elementary magnetic circuit model leading to Eq. 2, one expects no particular difficulties keeping β sufficiently small in the mass-minimized tuned scheme. For the tuned case, Eq. 2 can be put in the form

$$\beta = [(1 + K_1)\ K_m\ /\ K_c]^{1/2}\ R^{-1} + \ell \tag{40}$$

with the help of substitutions from Eqs. 25 and 5. For the parameters used in Fig. 5, one finds that $[(1+K_1)K_m/K_c]^{1/2}$=0.80, while the minimizing function R is plotted explicitly in Fig. 7 for several power levels. Thus roughly R$\sim$1.5, giving $\beta\sim$0.53; note that tuning reduces the sensitivity of β to α. The similarly behaving cylindrical model is expected to essentially support the same conclusions.

Except in the case of the nc magnet mass, the α at which the total specific mass is least can not be found by simple algebra in the present models. As previously discussed, this α may even be excluded by stability considerations. Nevertheless, the value of α for minimum M is relevant to design optimization studies. In contrast to treating α as a design degree of freedom, there exists an alternative approach in the nc case that prescribes α at the outset. Writing the nc load power as

$$P_r = V_{gen}\ I\ \alpha = \frac{V_{gen}^2}{X_s}\ \alpha\ \sqrt{1 - \alpha^2}\ , \tag{41}$$

one sees that at constant V_{gen}^2/X_s the P_r is maximum at $\alpha=1/\sqrt{2}$. Equivalently, the quantity $V_{gen}^2/(P_r\ X_s)$ is minimized. Based on this reasoning, an $\alpha=1/\sqrt{2}$ working rule has been used in linear alternator optimization studies.[6] To see this rule's significance in the present context, let us neglect ℓ and rearrange Eq. 2 into the form

$$\frac{V_{gen}^2}{P_r\ X_s} = \frac{M_m/P_r}{(1 + K_1)\ K_m}\ . \tag{42}$$

Hence at least for negligible ℓ, this rule for maximum P_r is equivalent to minimizing only the specific magnet mass M_m/P_r at constant $(1+K_1)K_m$. For as shown already, the α for least nc stator mass depends on the parameters and ratings, and hence does not follow this rule; Fig. 3 clearly shows that the minimum specific stator mass is generally not at $\alpha=1/\sqrt{2}$. As one considers progressively derated parameters, this rule can become even less relevant to minimum total mass. In the mass-minimized tuned cases computed, the minimum total mass was somewhere on the inductive branch, but never at resonance (α=1). However, the precise value of α for minimum M was not found.

One may of course deviate from minimum mass tuning, shifting more mass into core or coil such as to improve efficiency or to alter the magnet reaction or some other parameter. The only hard restriction is Eq. 8, i.e. the non-negativity of the capacitor mass. Although the sensitivity of the various parameters to such off-minimum deviation has not been studied, the equations developed here cover that mode as well.

Scaling Effects - Results and Discussion

A brief numerical investigation of the sensitivity to variations in some of the parameters was carried out to verify that the models produce physically reasonable magnitudes and trends. To this end, Fig. 8 is a repeat of Fig. 5A for a wide range of selected powers, extending from 12 kW to 100 kW. At constant α, the total specific mass decreases with increasing power in a way similar to the mass rule for an electric transformer.[7] Here, however, in the nc case a constant specific magnet mass, given by Eq. 36, gets added to the transformer-like stator specific mass given by the general form of Eq. 11. Inspection of Eqs. B14 and B8 reveals that M_s/P_r varies as $(J_r P_r^{1/3})^{-3/4}$ in the nc toroidal model and as $[J_r(P_r/L)^{1/2}]^{-2/3}$ in the nc cylindrical model. The s-dependence, residing in the function F(s) in Eq. 11, imposes additional modulation on these powers because s too is a function of exactly $J_r P_r^{1/3}$ or of $J_r(P_r/L)^{1/2}$, according to Eqs. 23 and 24, respectively. When capacitors are used the dependence on J_r and P_r remains as above. Even though then $P_t=DP_r/\alpha$ and s is given by either Eq. 27 or Eq. 28, the explicit form for D in Eq. 26 shows no dependence on J_r or P_r. Thus Fig. 8 also provides implicit information on the scaling of specific mass with J_r. This also shows that in the toroidal model the sensitivity of M_s/P_r to J_r exceeds its sensitivity to P_r by cubic power. Fig. 9 is presented to emphasize the generally great sensitivity of the total mass to current density.

The well known and substantial reduction in specific magnetics mass of alternators and transformers theoretically achievable by increasing the frequency can be thought of as due to reduced flux swing. In the toroidal model this effect varies as $f^{-3/4}$, while other effects of f get expressed through the shape scaling function s, the terminal volt·amperes in the tuned case, and the magnet mass. Examination of the frequency-resolved family of plots in Fig. 10 shows that for a fixed α near the minima a function of the form $af^{-3/4}+bf^{-1}$, with a and b constants, can approximate the nc ordinates quite well, at least over the limited frequency range. Mechanical limitations alone may make frequencies much in excess of 100 Hz impractical for 1-slot linear alternators rated tens of kW. And the potential mass savings can be lost if consequently B_s must be reduced in order to control core and stray eddy current losses. With regard to modest increases in frequency, the models on hand predict a mass reduction at nearly the -3/4 power. To ensure this, s, or equivalently the core-to-coil mass ratio, should not be allowed to deviate far from s_o, for otherwise F(s) will grow, tending to increase the mass. The nc toroidal formula for s, i.e. Eq. 23, indicates that to keep s fixed as ω increases, one must increase α such as to keep $\alpha/[\omega^{1/2}(1-\alpha^2)]$ a constant. This accounts for the shift to the right of the nc curve minima in Fig. 10. The nc magnet mass, being proportional to $1/(\omega\alpha\sqrt{1-\alpha^2})$, will then still decrease with increasing ω for

$\alpha > 1/\sqrt{2}$, although at a rate less than ω^{-1}; this is so because $\alpha\sqrt{1-\alpha^2}$ decreases with increasing α for $\alpha > 1/\sqrt{2}$. Qualitatively, to save mass, a higher frequency nc design should be at a lower β.

The shifting of the nc specific mass curve minima toward lower α with increasing power (Fig. 8) and toward higher α with increasing frequency (Fig. 10) results primarily from mass redistribution in the stator, and is effected through the argument P_r/ω of s. The s-related and physically more interesting core-to-winding mass ratio as given by

$$\frac{M_{core}}{M_{coil}} = \frac{\rho_c}{\rho_w} s^2 \tag{43}$$

for the toroidal case and by

$$\frac{M_{core}}{M_{coil}} = \frac{\rho_c}{\rho_w} (s^2 - 1) \tag{44}$$

for the cylindrical case. A plot of Eq. 43, with power as a parameter, is presented in Fig. 11. Its purpose is to support the model by showing that designs otherwise reasonable according to previous figures also produce reasonable mass ratios.

Reference designs by which to judge the absolute validity of this simplified modeling of a linear alternator are scarce in the literature. An existing 12.5 kW linear alternator labeled SPDE[9] and a paper study of a similar 25 kW one labeled RSSE[10] are described in unpublished reports. Both of these resonantly tuned machines were designed with the help of flux mapping codes, although not likely to the criteria invoked in this report. A design by Nasar and Chen[6] is based on detailed geometric approximation of flux paths[11], and is numerically optimized with respect to a weighted sum of mass and electrical losses, subject to $\alpha = 1/\sqrt{2}$ (cf. Eq. 41 and discussion) and to penalty functions on the constraints. Table I compares the results, available or estimated, for the above three machines with corresponding predictions by the toroidal and cylindrical models. These models do about equally well and best in regard to coil, magnet and capacitor masses, but they underestimate by a factor of 2 or so the core mass, the core-to-coil mass ratio and β. Underestimation of core mass is not surprising because the models assume a uniform stator flux density and no pole shoes. Shifting of mass between coil and core can also be due to weighting of efficiency or some unreported design criteria in the case of the SPDE and RSSE.

Magnet Utilization - Results and Discussion

The peak demagnetizing field that a magnet can tolerate before loss of intrinsic magnetic moment sets in is well known to decrease rapidly with rising temperature. At 300 °C even the presently available high energy 2-17 type Sm-Co magnets have usually lost over half of their room temperature intrinsic coercivity.[12,13] Therefore the demagnetizing field, or the corresponding dip (ΔB) of the B-field below B_r, is an important factor in evaluation and

comparison of alternator designs, especially at high temperature. The naive analysis of demagnetizing forces in Appendix A clearly falls short of accurately describing a magnet's field environment. Nevertheless the implications of this analysis are worth considering for they point up the consequent physics in a clear way. The expected result that a large magnet suffers little reaction is embodied in the equation

$$\frac{\Delta B}{B_r} = \frac{K_m}{1 + K} \cdot \frac{P_{gen}}{M_m} + \frac{K}{1 + K} , \tag{45}$$

which is a combination of Eqs. A27, A22 and A24. Then in the nc case Eq. 10 applies, giving

$$\frac{\Delta B}{B_r} = \frac{(\sqrt{1 - \alpha^2} - \ell)}{(1 + K)(1 + K_l)} + \frac{K}{1 + K} , \tag{46}$$

and in the tuned case all α dependence can be absorbed in $R(\alpha)$ by using Eqs. 25 and 5 to put Eq. 45 into the form

$$\frac{\Delta B}{B_r} = \frac{1}{(1 + K)\ R(\alpha)} \left[\frac{K_m}{(1 + K_l)\ K_c} \right]^{1/2} + \frac{K}{1 + K} . \tag{47}$$

In this analysis the part of a magnet under a stator pole face undergoes a reaction which is the sum of the gap reaction $K/(1+K)$ and a load power reaction, while the rest of the magnet is ignored. For large M_m the gap reaction predominates. As α is reduced in the nc case, the load reaction grows, but remains bounded. The behavior of the nc magnet reaction between its upper and lower bounds is presented in Fig. 12 for several values of the gap flux fringing ratio K_l and zero coil leakage ℓ. The influence of flux fringing on magnet reaction clearly diminishes with increasing α.

Another informative way to display the contents of Eq. 46 is to eliminate α by using Eq. 36 and plot $\Delta B/B_r$ against M_m/P_r, as is done in Fig. 13. The lower branch of this plot, where α is increasing and $\Delta B/B_r$ is decreasing with increasing M_m/P_r, is the one of interest if $\alpha > 1/\sqrt{2}$ is required.

When minimum mass capacitive tuning is implemented, the result is a magnet reaction less sensitive to α, because then R in Eq. 47 is not a strongly varying function of α (see Fig. 7). Using the cylindrical model and the previous reference set of parameters, Fig. 14 compares the α-sensitivity of $\Delta B/B_r$ of the nc to the tuned case for the same K_l. Although the capacitive branch has the lower magnet reaction corresponding to its greater magnet mass (cf. Fig. 5B), the reaction varies but little. In both cases the magnet reaction shown is well within the capabilities of modern, high-coercive rare earth-cobalt magnets, even at 300 °C.[13] A plot analogous to Fig. 13 can be done also for the minimum mass tuned case, but is not presented here.

High magnet temperature might require the reduction of the magnet reaction by upping the magnet mass, or conversely, one might decide to make the magnets

work harder by reducing their mass. In the nc case such freedom to alter the magnet mass at a fixed α does not exist, unless one changes the magnet height-to-width ratio a_h. If for some reason a lower α is unacceptable, then the only way to increase the normalized demagnetization reaction $\Delta B/B_r$ in Eq. 46 (or to decrease M_m/P_r in Eq. 36) is to reduce the gap flux fringing K_1 by decreasing a_h. Not much is gained once K_1 becomes small compared to unity, except that the magnet area A_m as well as the shape scaling s keep increasing (e.g., see Eqs. 21 and 23), making the magnets wafer-like and the stator heavier. For any fixed α in the tuned case, one has the extra freedom to trade off magnet mass versus capacitor mass in the inverse hyperbolic relation of Eq. 7, subject to the upper bound on magnet mass along the inductive branch imposed by Eq. 8. Keeping a_h fixed, one can easily decrease magnet size in this way to make them work harder at any α, but at the expense of deviating from minimum M. Also, as analyzed in Appendix C, s then decreases with decreasing R for large R and can even increase with decreasing R on intervals that depend on α and also on the model geometry. Instead of M, the R-freedom can thus be used to adjust some other s-sensitive quantity such as M_{core}/M_{coil}. Adjusting magnet mass in the tuned scheme by varying only the magnet height, and thus keeping the magnet area as well as s constant, is an interesting alternative which has not been fully investigated. Allowing a limited variation in a_h might be a feasible way to effect more control over the core-to-coil mass ratio and hence influence efficiency.

Conclusions

Based on idealized toroidal and cylindrical geometries, it was shown that the stator mass of an alternator designed to be capacitively tuned is always greater than the minimum achievable stator mass of an alternator designed with no capacitors (nc), assuming equal utilization of materials ratings, and the same frequency and power to a resistive load. This result can be attributed to an increase in the terminal volt-ampere product caused by a series capacitive reactance, which can, by design, either wholly or partially cancel, or even exceed, the internal inductive reactance of the alternator.

Use of the internal power factor (IPF=α) as a design degree of freedom was found to provide good clarification of various intricacies and options inherent in comparing the two approaches. Series capacitive tuning adds a degree of freedom which was expressed as a variation in the normalized magnet mass. This additional degree of freedom may then be used to minimize, at any α, say the total mass consisting of stator, the exciting permanent magnets and the capacitors. However, at power levels of tens of kW, the stator mass is by far the greater and hence tends to dominate the behavior of the total mass. In the nc case, the α for minimum specific stator mass was found to generally vary with the parameters and ratings, whereas the minimum specific magnet mass is at $\alpha=1/\sqrt{2}$. The α of the tuned case total mass minimum likewise varies, and is never at resonance. In the nc case both stator and magnet specific masses are unbounded as $\alpha \to 1$, but in the tuned case all masses remain finite. Moreover, in the tuned case, the magnet plus capacitor mass varies at a less than proportional rate with the capacitor specific mass (see Eq. 37). Therefore on the basis of this study, costly efforts to reduce capacitor mass would seem to be unwarranted.

Unless possible external constraints are considered, such as driving engine stability or deratings arising from high temperature, this study can find no apparent advantage in capacitive tuning. With no such special constraints or deratings, any overall mass advantage of a tuned design is entirely negligible. However, a slight reduction in magnet mass for the tuned case could improve stability and reduce windage losses, but at the expense of load fault effects and capacitor reliability. When an upper bound is invoked on the ratio (β) of the inductive voltage drop in the alternator to its internal emf, the nc approach still seems to be favored. This bound, which assures stability of oscillation for an FPSE-linear alternator system, has been reported to be the lowest in the nc case. For example, in the nc case an α of 0.9 is sufficient to satisfy the lowest quoted value of 0.5 for the β limit. Indeed, with realistic ratings and for α=0.9, the mass savings resulting from tuning amount to only a few percent. Serious deratings, such as a magnet remanence reduced to 0.7 T and a stator magnetic saturation reduced to 1 T, are needed for tuning to save about 16%. Unless the deratings are rather severe, one would likely not opt for the undesirable bulk of extra hardware and potentially serious reliability problems introduced by tuning capacitors. Safety considerations may require the use of active feedback control to reinforce the otherwise rather marginal amplitude stability of high power FPSE thermodynamic oscillators[14]. Active feedback control may then raise the nc case β limit, further favoring no tuning.

The exciting magnet reaction $\Delta B/B_r$ due to the applied demagnetizing field has been analyzed as a sum of elementary magnet gap and load power components. While the self-demagnetizing influence due to the gap is clearly the minimum possible $\Delta B/B_r$, there is also a bound on the maximum $\Delta B/B_r$ in the nc case (see Eq. 46). Since an nc design will likely have an $\alpha \geq 1/\sqrt{2}$, this condition selects that, or lower, branch of the curve shown in Fig. 13, where the magnet reaction is monotonically decreasing with increasing specific magnet mass. Therefore the best that can be done in the nc approach to minimize magnet mass, should that in itself matter, is to approach either the magnet reaction or stability limits, should the corresponding limits on M_m exceed the absolute lower bound on M_m at $\alpha = 1/\sqrt{2}$. In the tuned case it is theoretically possible, at any given α, to arbitrarily reduce the magnet mass, but then the capacitor mass, the coil-to-core mass ratio, and the total mass all increase without bound. An alternative way to adjust the tuned case magnet mass while asserting more control over variation of the other masses may be to also allow some simultaneous adjustment in the a_h. Varying magnet height with area fixed is an interesting special case of such possibilities which need further investigation. At each α, that magnet mass which minimizes the total mass, including capacitors, was shown to be well defined and computable. The resulting normalized demagnetizing reaction $\Delta B/B_r$ for these αs was shown to be acceptable for both the mass-minimized tuned and nc cases; indeed, the values of $\Delta B/B_r$ computed in examples were all less than unity, and hence well within the capability of modern, high-coercive 2-17 type samarium cobalt magnets, even at 300 °C.

Algebraic modeling equations were developed to generate comparative plots of the various alternator component masses as functions of the free variables. It has been shown that the stator mass can be expressed as a product of a transformer-like term, involving the terminal volt·ampere product raised to a geometry dependent fractional power, and a simple algebraic function of a ratio

s scaling the shape. s in turn uniquely determines the core-to-coil mass ratio and is itself an algebraic function of the ratings and free variables. This approach of grouping of terms makes possible some intuitive penetration of the complexities of the many variables which determine the total mass and its distribution. Then various scaling effects, couplings, sensitivities and trends become apparent, which, rather than computation of actual designs, is the real advantage of the method. Finally, this approach may be useful to clarify scaling effects, sensitivities and trends in other alternator characteristics, such as the efficiency, that strongly depend on mass and its distribution.

Symbols and Abbreviations

a_h - magnet height-to-width ratio

a_w - coil wire conductor cross-section (m^2)

A_m - cross-section of magnets of any one orientation (m^2)

A_p - a constant defined by Eq. B8 (m^4/W)

A_s - cross-section of stator core (m^2)

B - magnetic flux density (T)

B_1, B_2 - flux density in magnets no. 1, 2 (T)

B_r - magnet remanence (T)

B_s - peak flux density in stator (T)

C - capacitance of tuning capacitor (F)

D - a function defined by Eq. 17

$D_\pm$ - D evaluated for inductive (−) or capacitive (+) IPF branch

f - frequency (Hz)

$f_\pm(R)$ - functions defined by Eqs. C1 and C7

F - a function defined in Eq. 11

h_g - total height of gap between magnet and pole faces (m)

h_m - magnet height (m)

H - magnetic field intensity (A/m)

H_1, H_2 - field intensity in magnets no. 1, 2 (A/m)

H_{min} - minimum (most negative) field intensity in a magnet (A/m)

H_s - field intensity in stator core (A/m)

$i(t)$ - instantaneous alternator current (A)

I - rms alternator current (A)

$\tilde{I}$ - complex vector rms alternator current (A)

IPF - internal power factor of alternator

I_r - rated rms alternator current (A)

J_r - rated rms current density in coil wire (A/m^2)

K - a constant defined by Eq. A6

K_1 - ratio of stator gap fringing flux to magnet flux under a stator pole face, defined by Eq. A18

K_c - capacitor specific mass, a constant defined by Eq. 1 (kg/(V A))

K_g - ratio of gap height h_g to magnet height h_m

K_l - ratio of stator gap fringing flux to flux under a stator pole face, with magnets absent

K_m - a constant defined by Eq. A24 (kg/W)

K_w - ratio of coil cross-section to total conductor cross-section

ℓ - ratio of coil leakage inductance drop to V_{gen}

l - length of magnet in direction transverse to motion (m)

l_s - mean magnetic path length of stator core (m)

$\bar{l}$ - mean length of bordering strip used to estimate gap fringing flux (m)

L - length of coil in the cylindrical model (m)

L_{lc} - coil leakage inductance (H)

L_{lg} - stator gap leakage, or fringing, inductance with magnets present, as defined by Eq. A12 (H)

L_m - magnet reaction inductance, with magnets in stator gap, (H)

L_s - total equivalent series inductance of alternator (H)

M - total mass, $M_s+M_m+M_c$, of alternator (kg)

M_c - mass of capacitor (kg)

$M_{c\pm}$ - M_c evaluated for the inductive (−) or capacitive (+) IPF branch (kg)

M_{coil} - mass of stator coil (kg)

M_{core} - mass of stator core (kg)

M_m - total mass of magnets (kg)

M_{mo} - magnet mass for minimum M_m+M_c, defined by Eq. 5 (kg)

M_s - mass of stator, $M_{core}+M_{coil}$, (kg)

nc - designates no-capacitor case

N - number of turns in stator coil

p - a constant defined by Eq. A7

P_c - volt-ampere product for capacitor (V A)

P_{gen} - volt-ampere product for alternator (V A)

P_r - rated alternator power to a resistive load (W)

P_t - terminal volt-ampere product of alternator under load (V A)

r_1 - radius of coil cross-section, toroidal or cylindrical model (m)

r_2 - radius (outer radius) of core in toroidal (cylindrical) model (m)

r_m - magnet radius in toroidal model (m)

R - normalized magnet mass, M_m/M_{mo}

R_l - load resistance (Ω)

R_s - series resistance representing alternator electrical losses (Ω)

R_g, R_{g1}, R_{g2}, R_{lc}, R_{lg}, R_m, R_{m1}, R_{m2}, R_s - reluctances, see Appendix A

$R_{0\pm}$ - roots given by Eq. C9

s - alternator model shape scaling ratio r_2/r_1

s_o - value of s giving minimum stator mass for constant P_t

$v_{gen}(t)$ - instantaneous internal emf, or open circuit terminal voltage, of alternator (V)

$v_t(t)$ - instantaneous terminal voltage of alternator under load (V)

V_{gen} - rms internal emf, or open circuit terminal voltage, of alternator (V)

$\tilde{V}_{gen}$ - complex vector rms internal emf of alternator (V)

V_{lc}, V_{lg}, V_{Lm}, V_{Ls} - rms voltage drop across coil leakage, stator gap fringing, magnet reaction and total series inductance, respectively (V)

$\mathcal{V}_m$ - total volume of magnets of any one orientation (m^3)

V_t - rms terminal voltage of alternator under load (V)

w - width of magnet, or alternator plunger stroke (m)

$x(t)$ - instantaneous alternator plunger position (m)

x_o - amplitude of alternator plunger oscillation (m)

X_s - total inductive reactance ωL_s of alternator (Ω)

α - short symbol for the IPF

β - ratio of alternator inductive voltage drop to V_{gen}

ϵ - a constant defined by Eq. C2

$\gamma_{\pm}$ - constants defined by Eq. 6

ΔB - peak demagnetizing flux density swing (T)

μ_m - permeability ($\mu_o \mu_{mr}$) of magnet (H)

μ_{mr} - relative permeability of magnet

μ_o - permeability of vacuum, $4\pi 10^{-7}$H

ρ_c - density of stator core (kg/m^3)

ρ_{cu} - density of copper (kg/m^3)

ρ_m - density of magnet (kg/m^3)

ρ_w - density of stator coil, averaged over wire and insulation (kg/m^3)

$\phi_c(t)$ - instantaneous flux through stator coil (Wb)

$\phi_{lc}(t)$ - instantaneous coil slot leakage flux (Wb)

$\phi_{lg}(t)$ - instantaneous magnet gap fringing flux (Wb)

$\phi_m(t)$ - instantaneous total flux contributed by the magnets (Wb)

$\phi_s(t)$ - instantaneous stator pole flux (Wb)

ω - angular frequency $2\pi f$ (sec^{-1})

REFERENCES

1. Fitzgerald, A.E.; Kingsley, C.; and Umans, S.D.: Electric Machinery. Fourth ed., McGraw-Hill, Inc., 1983, ch. 7.

2. Slaby, J.G.: Free-Piston Stirling Technology for Space Power. NASA TM-101956, 1989.

3. Wieserman, W.: Private communication. Univ. of Pittsburgh at Johnstown.

4. Nasar, S.A.; and Chen, C.: Magnetic Circuit Analysis of a Tubular Permanent Magnet Linear Alternator. Elec. Machines and Power Systems, vol. 13, no. 6, 1987, pp. 361-371.

5. Mechanical Technology, Inc., et al.: Conceptual Design of an Advanced Stirling Conversion System for Terrestrial Power Generation. NASA CR-180890, DOE/NASA/0372-1, 1988.

6. Nasar, S.A.; and Chen, C.: Optimal Design of a Tubular Permanent Magnet Linear Alternator. Elec. Machines and Power Systems, vol. 14, nos. 3-4, 1988, pp. 249-259.

7. Schwarze, G.E.: Development of High Frequency Low Weight Power Magnetics for Aerospace Power Systems. Proc. of the 19th Intersociety Energy Conversion Engineering Conf., vol. 1, Aug. 1984, pp. 196-204. NASA TM-83656.

8. MIT Elec. Engineering Staff: Magnetic Circuits and Transformers. John Wiley & Sons, Inc., 1943, ch. 3.

9. Mechanical Technology, Inc.: SPDE Phase I Final Report. NASA CR-179555, 1987.

10. Mechanical Technology, Inc.: RSSE Design Status - Internal Review. Nov. 7, 1989, unpublished.

11. Nasar, S.A.; and Chen, C.: Inductance and the Leakage Field of a Tubular PM Linear Alternator. Elec. Machines and Power Systems, vol. 14, no. 1, 1988, pp. 83-94.

12. Potenziani, E., II, et al.: The Temperature Dependence of the Magnetic Properties of Commercial Magnets of Greater than 25 MGOe Energy Product. J. Appl. Phys., vol. 57, no. 8, pt. IIB, Apr. 15, 1985, pp. 4152-4154.

13. Niedra, J.M.; and Overton, E.: 23 to 300 °C Demagnetization Resistance of Samarium-Cobalt Permanent Magnets. NASA TP-3119, 1991.

14. Redlich, R.W.; and Berchowitz, D.M.: Linear Dynamics of Free-Piston Stirling Engines. Proc. Inst. Mech. Eng., vol. 199, no. A3, Mar. 1985, pp. 203-213.

Appendix A

Internal EMFs, Magnet Size, and Demagnetizing Forces

Basic magnetics equations are applied to the model shown in Fig. A1 in order to relate exciting magnet size to equivalent circuit parameters, power and demagnetizing fields. A pair of oppositely polarized magnets moves between the poles of a magnetic core made of some magnetically soft laminations. This closed magnetic circuit links an N-turn armature coil, not shown, which supplies power to a load. The path P_1 following the magnetic circuit may in fact intercept another such pole face and magnet pair arrangement before closing on itself; however, in such a case h_m and h_g represent the total length of magnet and length of air gap, respectively, in the circuit, and the magnet pairs are assumed to be mechanically linked.

Internal EMFs and Equivalent Circuit

Summation of mmf around P_1 couples the magnet field H_2, the stator field H_s, the gap flux density B_2 and the instantaneous current i according to

$$H_2\, h_m + \frac{B_2}{\mu_o}\, h_g + H_s\, l_s + N\, i = 0 \ . \tag{A1}$$

Similarly, path P_2 couples the magnet fields to each other according to

$$(H_1 + H_2)\, h_m + (B_1 + B_2)\, h_g \,/\, \mu_o = 0 \ . \tag{A2}$$

And the total flux contributed by the magnets is the sum

$$\phi_m = l(w/2 + x)\, B_2 - l(w/2 - x)\, B_1 \ , \tag{A3}$$

where $lw=A_m$ is the total cross-section of magnets of any one orientation. Thus, fringing fields in the region between adjacent but oppositely oriented magnets have been ignored. Moreover, flux fringing around the ends of the magnets and "leaking" around the coil in its vicinity can at best be only estimated, unless one computes the fields of specific geometries. Here formal symbols R_{lg} and R_{lc} will be assigned to these gap and coil leakage reluctances.

High energy rare earth-cobalt magnets of the type assumed here are well characterized by

$$B = \mu_m\, H + B_r \tag{A4}$$

in a cyclically driven mode along the recoil line in their normal quadrants of operation, where $\mu_m=\mu_{mr}\,\mu_o$ in the SI units. In this mode their relative permeability μ_{mr} is slightly above unity and their remanence B_r is about 1 T.

To utilize the algebraic facility provided by the flux-reluctance-mmf notation, the magnetic circuit is modeled as shown in Fig. A2. In the present case a magnet is equivalent to a magnetic potential generator of strength $h_m B_r/\mu_m$ in series with a position-sensitive reluctance $[R_{mi}(x)+R_{gi}(x)]$, $i=1,2$, of the part of its body under a pole face of the stator. Otherwise the notation is standard, and a list of reluctances is defined below, where numerical subscripts appearing on the position-sensitive reluctances refer to either magnets no. 1 or no. 2:

$$R_{m1} = \frac{h_m}{\mu_m \, l \, (w/2 - x)} , \qquad \text{(body reluctance under the stator, magnet no. 1)}$$

$$R_{m2} = \frac{h_m}{\mu_m \, l \, (w/2 + x)} , \qquad \text{(body reluctance under the stator, magnet no. 2)}$$

$$R_{g1} = \frac{h_g}{\mu_o \, l \, (w/2 - x)} , \qquad \text{(gap reluctance under the stator, magnet no. 1)}$$

$$R_{g2} = \frac{h_g}{\mu_o \, l \, (w/2 + x)} , \qquad \text{(gap reluctance under the stator, magnet no. 2)}$$

$$R_s = \frac{l_s}{\mu_s \, A_s} , \qquad \text{(linearized stator reluctance)}$$

R_{lg} = reluctance to measure flux fringing around the magnets,

R_{lc} = coil leakage reluctance,

$R_g = \dfrac{h_g}{\mu_o \, A_m}$ = total gap reluctance,

$R_m = \dfrac{h_m}{\mu_m \, A_m}$ = total reluctance of magnet material in gap.

Further refinements to this circuit are possible, such as introducing a leakage path between the junction of R_{mi} and R_{gi} to the opposite side of the flux generator, but will not be pursued here.

Using Fig. A2 and successive Thevenin equivalent reductions or else loop equation algebra, one finds the instantaneous flux in the coil to be

$$\phi_c(t) = \frac{2 \, A_m \, B_r \, x(t)}{p \, w} - \left[\frac{(1 + K)}{p \, R_{lg}} + \frac{1}{p \, R_m} + \frac{1}{R_{lc}} \right] N \, i(t) , \qquad \text{(A5)}$$

where

$$K \equiv \mu_{mr} K_g \equiv \mu_{mr} h_g / h_m , \tag{A6}$$

and

$$p \equiv (1 + K) (1 + R_s / R_{lg}) + R_s / R_m . \tag{A7}$$

In a well designed machine the stator will utilize a magnetically soft material that will not be driven into hard saturation. Therefore normally $R_s \ll R_{lg}$ and $R_s \ll R_m$, making

$$p \approx 1 + K \tag{A8}$$

a very good approximation.

Eq. A5 presents a useful decomposition of the total coil flux because its time derivative gives the instantaneous terminal voltage $v_t(t)$ as a sum of terms that have standard interpretations in alternator theory:

$$v_t(t) = N \frac{d\phi_c}{dt} = v_{gen}(t) - (L_{lg} + L_m + L_{lc}) \frac{di}{dt} , \tag{A9}$$

where

$$v_{gen}(t) = N \frac{2 A_m B_r}{p w} \cdot \frac{dx}{dt} \tag{A10}$$

is the internal generator or no-load terminal voltage,

$$L_{lg} = \frac{(1 + K) N^2}{p R_{lg}} \tag{A11}$$

is the stator gap leakage or fringing inductance with magnets present,

$$L_m = \frac{N^2}{p R_m} \tag{A12}$$

is the magnet reaction inductance for magnets in the stator gap, and

$$L_{lc} = \frac{N^2}{R_{lc}} \tag{A13}$$

is the coil leakage inductance. For the usual case of sinusoidal x(t) with amplitude x_o the corresponding rms V_{gen} is

$$V_{gen} = N \frac{\sqrt{2} A_m B_r \omega}{p w} x_o , \tag{A14}$$

where in normal operation $x_o = w/2$. Hence forth all voltage and current symbols

will denote sinusoidal rms values. This then establishes the correspondence to the alternator lumped equivalent circuit shown in Fig. 1.

Of the three load current induced voltages in Eq. A9 , namely

$$V_{Lm} = \omega L_m I ,$$
$$V_{lg} = \omega L_{lg} I , \qquad (A15)$$
$$V_{lc} = \omega L_{lc} I ,$$

only V_{Lm} is completely determined at this point. The L_{lc} is rather dependent on the shape of the coil and its surrounding slot. Since slot and coil geometry are not the objectives of this study, L_{lc} will be considered an unknown value controllable to a negligible value by good design practices, and the symbol

$$\ell \equiv V_{lc} / V_{gen} \qquad (A16)$$

will be carried for completeness only. On the other hand, the L_{lg} is much more significant because driven by the mmf Ni, a substantial amount of flux will fringe around the magnets if the magnet height-to-width ratio is not small. Resorting to one of the standard approximations is most expeditious, and we shall assume R_{lg} to be the reluctance of a cylinder of height (h_m+h_g) and cross-section of a strip of width $(h_m+h_g)/2$ bordering the periphery of the magnet gap.[8] If $\bar{l}$ denotes the mean length of the strip, then this prescription gives

$$R_{lg} = 2 / (\mu_o \bar{l}) . \qquad (A17)$$

Introduction of the slightly permeable magnet material between the pole faces decreases slightly the fringing of flux around the volume between the faces. The ratio of fringing flux to magnet area flux becomes

$$K_1 \equiv L_{lg}/L_m = (1 + K) R_m / R_{lg}$$
$$= \frac{(1/\mu_{mr} + K_g)}{(1 + K_g)} \cdot K_l , \qquad (A18)$$

where K_l is the ratio of fringing to central area flux for a free space gap. Hence K_l can be found from a given $a_h=h_m/w$ and pole face shape. In the above stated prescription for fringing,

$$K_l = \frac{\bar{l} (h_m + h_g)}{2 A_m} . \qquad (A19)$$

The ratio of the sum of the three inductive drops listed in Eq. A15 to V_{gen} can now be written as

$$V_{Ls}/V_{gen} = [(1 + K_1)\ V_{Lm}/V_{gen}] + \ell\ , \tag{A20}$$

having used the definitions in Eqs. A16 and A18. Finally from Eqs. A12, A14, the first of A15 and the definition of R_m follows the useful expression

$$V_{Lm}/V_{gen} = \frac{2\ p\ \mu_m\ P_{gen}}{\omega\ \mathcal{V}_m\ B_r^2}\ , \tag{A21}$$

where $\mathcal{V}_m$ is the volume of magnets of one orientation and P_{gen} is the volt·ampere product of the machine. From the total magnet mass

$$M_m = 2\ \rho_m\ \mathcal{V}_m \tag{A22}$$

follows the alternative form

$$V_{Lm}/V_{gen} = K_m\ P_{gen}\ /\ M_m \tag{A23}$$

of Eq. A21, where the inverse of the constant

$$K_m \equiv \frac{4\ p\ \rho_m\ \mu_m}{\omega\ B_r^2} \tag{A24}$$

is proportional to the energy per unit mass of the magnets times the frequency.

Suppose next that a second identical stator gap and a magnet pair mechanically linked to the first pair are introduced into the magnetic circuit, as in some existing designs. This is equivalent to doubling the h_m and h_g of the single gap circuit, provided the R_{Lg} is also doubled. This can be seen by inspection or shown by equivalent circuit algebra. The formulas A20 through A24 remain valid provided $\mathcal{V}_m$ and M_m remain as defined, which thus doubles their values. Clearly K is unchanged, but R_m is doubled. It follows then from Eq. A18 that K_1 remains invariant. Indeed, one can see that for most quantities of practical interest this transformation is completely described by $a_h \rightarrow 2a_h$.

Demagnetizing Forces

It remains yet to establish the relation of the field swing amplitude in the magnets to their volume, or mass, and P_{gen}. To this end the circuit in Fig. A2 gives the rather tedious exact solution

$$H_2(t) = -\frac{K\ B_r}{\mu_m\ (1 + K)} - \frac{N\ i(t)}{p\ h_m} - \frac{(R_s/R_m)\ (B_r/\mu_m)\ [2\ x(t)/w]}{(1 + K)\ p} \tag{A25}$$

for the instantaneous field in magnet no. 2. As before, the last group of

terms can be dropped because (R_s / R_m) is assumed to be very small. Moreover, any part of a magnet not under a pole face is subject to different demagnetizing forces and influences the other part still in the gap. Therefore the value of the above equation may lie mostly in that it accounts for the effect of load current and air gap on the part of a magnet under a pole face, where demagnetizing influences seem likely to be the most severe.

The minimum, or most negative, value of H_2 in Eq. A25 occurs for peak positive i, which is $\sqrt{2}$ I in the sinusoidal case. Thus any magnet part under a pole face will experience a peak demagnetizing field of about

$$H_{min} = - \frac{K B_r}{\mu_m (1 + K)} - \frac{N \sqrt{2} I}{h_m (1 + K)} . \tag{A26}$$

If N is eliminated with the help of Eq. A14, then the result can be put in the form

$$\frac{P_{gen}}{2 \mathcal{V}_m} = - \frac{\omega B_r^2}{4 \mu_m} \left(\frac{\mu_m H_{min}}{B_r} + \frac{K}{1 + K} \right), \tag{A27}$$

where $2\mathcal{V}_m$ is the total magnet volume. Note that this gives an interesting alternative version of Eq. A23:

$$V_{Lm}/V_{gen} = - (1 + K) \left(\frac{\mu_m H_{min}}{B_r} + \frac{K}{1 + K} \right). \tag{A28}$$

This result can be substituted directly into Eq. A20 in order to express V_{Ls}/V_{gen} too as a function of the peak demagnetizing field. In this paper, when dealing with the peak demagnetizing field, instead of H_{min}, reference will usually be made to the corresponding dip ΔB of the B-field in the magnets below the remanence B_r. It is defined as the positive quantity

$$\Delta B \equiv -\mu_m H_{min} . \tag{A29}$$

Appendix B

Stator Mass for Toroidal and Cylindrical Configurations

The toroidal stator geometry, drawn in Fig. B1, consists of a magnetic core torus, of window radius r_1 and cross-section radius r_2, interlocked with a coil torus which fills the core window completely. Hence the coil window has radius r_2 and the coil cross-section has radius r_1. The cylindrical geometry, drawn in Fig. B2, consists of a magnetic core in the shape of a long pipe whose bore is filled with coil wire running lengthwise. The cylinder's inner radius is r_1, outer radius is r_2 and length is L. One can imagine, if desired, that this pipe makes a loop, closing on itself. Exciting magnets may be thought of as existing in appropriately located gaps in these magnetic circuits, but which are ignored for present purposes. In fact, this omission may improve approximation to reality because the extra magnetic circuit length needed to accommodate magnet height is not useable for additional coil cross-section in the referenced tubular linear alternators[2,4]. These particular geometries are interesting in that their contrasting symmetry generates rather different functions to test the sensitivity to alternator configurations.

(I) Interlocked Toroids

Stator mass M_s is the sum of the magnetic core mass

$$M_{core} = 2\,\pi^2\,(r_1 + r_2)\,r_2^{\,2}\,\rho_c \qquad (B1)$$

and coil mass

$$M_{coil} = 2\,\pi^2\,(r_1 + r_2)\,r_1^{\,2}\,\rho_w\ , \qquad (B2)$$

where ρ_c is the core density and ρ_w is the coil density averaged over wire and insulation. Denoting the wire conductor cross-section by a_w, one can account for insulation and space by writing $K_w a_w$, with $K_w>1$, for the total area per wire. Thus the coil has

$$N = \frac{\pi\ r_1^{\,2}}{K_w\ a_w} \qquad (B3)$$

turns, and in case of copper wire insulated by a much lighter material, a density

$$\rho_w \approx \rho_{cu}\ /\ K_w\ . \qquad (B4)$$

As the magnetic flux density in the core oscillates with maximum permissible amplitude B_s, the rms terminal voltage is found from $Nd\phi_c/dt$ to be

$$V_t = \frac{N\,\omega\,B_s\,\pi\,r_2^2}{\sqrt{2}} = \frac{\omega\,B_s}{\sqrt{2}\,K_w\,a_w}\,(\pi\,r_1\,r_2)^2\ , \tag{B5}$$

with N finally eliminated by use of Eq. B3. And the current is at its rated value

$$I_r = a_w\,J_r\ , \tag{B6}$$

as limited by the maximum permissible rms current density J_r. Then the terminal volt-ampere product is

$$P_t = V_t\,I_r = (\pi\,r_1\,r_2)^2\ /\ A_p\ , \tag{B7}$$

where

$$A_p \equiv \frac{\sqrt{2}\,K_w}{\omega\,B_s\,J_r}\ . \tag{B8}$$

It is convenient to express all masses and dimensions in terms of A_p, P_t and a dimensionless scaling ratio

$$s \equiv r_2\ /\ r_1\ . \tag{B9}$$

Using Eqs. B7 and B9 one finds

$$r_1 = \pi^{-1/2}(A_p\,P_t)^{1/4}\,s^{-1/2}\ , \tag{B10}$$

$$r_2 = \pi^{-1/2}(A_p\,P_t)^{1/4}\,s^{1/2}\ . \tag{B11}$$

The desired mass formulas follow immediately from Eqs. B1, B2, B10 and B11:

$$M_{core} = 2\,\pi^{1/2}\,\rho_c\,(A_p\,P_t)^{3/4}\,(1+s)\,s^{1/2}\ , \tag{B12}$$

$$M_{coil} = 2\,\pi^{1/2}\,\rho_w\,(A_p\,P_t)^{3/4}\,(1+s)\,s^{-3/2}\ , \tag{B13}$$

giving the stator mass

$$M_s \equiv M_{core} + M_{coil} = 2\,\pi^{1/2}\,(A_p\,P_t)^{3/4}\,(1+s)\,(\rho_c\,s^{1/2} + \rho_w\,s^{-3/2})\ . \tag{B14}$$

For constant P_t the $M_s(s)$ has a minimum at the sole real positive root s_o of

$$(3\,s+1)\,s^2 - (s+3)\,\rho_w/\rho_c = 0\ . \tag{B15}$$

For example, if $\rho_w=\rho_c$ then $s_o=1$, giving $M_{core}=M_{coil}$, or if $\rho_c=2\rho_w$ then $s_o\approx0.7576$ and $M_{core}=1.15M_{coil}$.

(II) Long Pipe

This geometry can be conveniently normalized with respect to its length L. Otherwise the formulas are developed in the same way as in (I) above, and they will be listed without further discussion and labeled by priming the corresponding formula numbers of (I). Formulas which are the same as in (I) are omitted.

$$M_{core}/L = \pi\ (r_2^2 - r_1^2)\ \rho_c\ , \tag{B1'}$$

$$M_{coil}/L = \pi\ r_1^2 \rho_w\ , \tag{B2'}$$

$$V_t/L = \frac{\omega\ B_s}{\sqrt{2}\ K_w\ a_w} \cdot \pi\ r_1^2\ (r_2 - r_1)\ , \tag{B5'}$$

$$P_t/L = \pi\ r_1^2\ (r_2 - r_1)\ /\ A_p\ , \tag{B7'}$$

$$r_1 = (A_p/\pi \cdot P_t/L)^{1/3}\ (s - 1)^{-1/3}\ , \tag{B10'}$$

$$r_2 = (A_p/\pi \cdot P_t/L)^{1/3}\ s\ (s - 1)^{-1/3}\ , \tag{B11'}$$

$$M_{core}/L = \pi^{1/3}\ \rho_c\ (A_p\ P_t/L)^{2/3}\ (s - 1)^{1/3}\ (s + 1)\ , \tag{B12'}$$

$$M_{coil}/L = \pi^{1/3}\ \rho_w\ (A_p\ P_t/L)^{2/3}\ (s - 1)^{-2/3}\ , \tag{B13'}$$

$$M_s/L = \pi^{1/3}\ (A_p\ P_t/L)^{2/3}\ (s - 1)^{-2/3}\ [(s^2 - 1)\ \rho_c + \rho_w]\ . \tag{B14'}$$

For constant P_t/L the $M_s(s)/L$ has a minimum at the sole root $s_o>1$ of

$$s^2 - 3s/2 + (1 - \rho_w/\rho_c)/2 = 0\ , \tag{B15'}$$

which is

$$s_o = 3/4 + (1 + 8\ \rho_w/\rho_c)^{1/2}/4.$$

Note that in this geometry $\rho_w=\rho_c$ gives $s_o=3/2$ and $M_{core}=1.25M_{coil}$. One could say that with respect to distribution of coil versus stator mass the cylindrical geometry has an inherent bias.

Appendix C

Variation of s with R in the Tuned Case

In the tuned case one has the additional freedom to vary the magnet mass or, equivalently, R at a fixed α and ratings. This variation induces variations in s-sensitive quantities such as M_s and M_{core}/M_{coil} because s is a strong function of R. A qualitative understanding of the dependence of s on R is therefore useful, but is not apparent from a cursory inspection of Eq. 27 or Eq. 28 because the D-factor involves R in an inhomogeneous way. Therefore a brief analysis of this dependence is presented for the case of variation of R at constant a_h.

A. Toroidal geometry:

In this case, by Eq. 27, $s_{\pm}^2$ is proportional to $R^{4/3}\ D_{\pm}$, where $D_{\pm}^2$ is given by Eq. 26. Is $s_{\pm}^2$, or equivalently $R^{4/3}\ D_{\pm}$, then a monotonic function of R? To answer this, it is convenient to study instead the functions

$$f_{\pm}(R) \equiv R^{8/3}\ D_{\pm}^2(R) = \alpha^2\ R^{8/3} + \epsilon\ R^{2/3}\ (1 + \gamma_{\pm}\ R)^2\ , \tag{C1}$$

where

$$\epsilon \equiv (1 + K_1)\ K_m\ /\ K_c. \tag{C2}$$

γ_+, as defined by Eq. 6, is a manifestly non-negative quantity. Hence $f_+(R)$ is a sum of positive terms each monotonically increasing with R. Therefore s_+^2 is monotonically increasing with R.

The case of s_-^2 requires detailed examination because γ_- may be, and usually will be, negative. This case can be understood by examining the derivative

$$f_-'(R) = (1/3)\ R^{-1/3}\ [4(\alpha^2 + \epsilon\gamma_-^2)R^2 + 5\epsilon\gamma_- R + \epsilon] \tag{C3}$$

for changes of sign, for s_-^2 is monotonic on any interval where $f_-'(R)$ is of constant sign. Assuming ℓ=0,

$$\alpha^2 + \epsilon\gamma_{\pm}^2 = 1 \tag{C4}$$

holds identically and Eq. C3 simplifies to

$$f_-'(R) = (1/3)\ R^{-1/3}\ (4R^2 - 5\epsilon^{1/2}\sqrt{1 - \alpha^2}\ \ R + \epsilon)\ . \tag{C5}$$

For α>3/5 the quadratic form in R on the RHS of Eq. C5 is positive definite, making $f_-'(R)$>0 for all R>0. For α<3/5 this quadratic form has 2 positive roots, making $f_-'(R)$<0 for

$$(5/8)\epsilon^{1/2}(\sqrt{1 - \alpha^2} - \sqrt{(9/25) - \alpha^2}\ ) < R < (5/8)\epsilon^{1/2}(\sqrt{1 - \alpha^2} + \sqrt{(9/25) - \alpha^2}\ ). \tag{C6}$$

Thus in the ℓ=0 case, the s_-^2 is monotonically increasing for all R if α>3/5. But if α<3/5, then s_-^2 is monotonically increasing for all R except on the interval C6, where s_-^2 is monotonically decreasing with R. The ℓ>0 case can be analyzed similarly.

B. Cylindrical geometry:

In this case, by Eq. 28, $(s_\pm - 1)^2$ is proportional to $R^{3/2}D_\pm^2$, but from the point of view of Eq. 44 the interest is in $(s_\pm^2 - 1)$. However, it is apparent that if one of the quantities $s_\pm$, $(s_\pm - 1)^2$ or $(s_\pm^2 - 1)$ is monotonic, then so are they all; e.g., $s^2 - 1 = (s - 1)^2 + 2(s - 1)$. Hence it is sufficient to study the monotonicity of

$$f_\pm(R) \equiv R^{3/2}\, D_\pm^2(R) = R^{3/2}\, [\alpha^2 + \epsilon(R^{-1} + \gamma_\pm)^2] \ . \tag{C7}$$

Again we examine the derivative

$$f_\pm'(R) = (1/2)\, R^{-3/2}\, [3(\alpha^2 + \epsilon\gamma_\pm^2)R^2 + 2\epsilon\gamma_\pm R - \epsilon] \tag{C8}$$

for changes of sign. For both γ_+ and γ_- the RHS of Eq. C8 has always one positive and one negative root given by

$$R_{0\pm} = \frac{-\epsilon\gamma_\pm \oplus [(\epsilon\gamma_\pm)^2 + 3\epsilon(\alpha^2 + \epsilon\gamma_\pm^2)]^{1/2}}{3(\alpha^2 + \epsilon\gamma_\pm^2)} \ , \tag{C9}$$

where the symbol $\oplus$ labels the positive and the negative roots. In the case ℓ=0, Eq. C4 applies, showing that $f_\pm'(R)$>0 (i.e., $f_\pm(R)$ is monotonically increasing) iff R>$R_{0\pm}$, and that $f_\pm'(R)$<0 (i.e., $f_\pm(R)$ is monotonically decreasing) iff R<$R_{0\pm}$, where

$$R_{0\pm} = (1/3)\, \epsilon^{1/2}\, (\mp\sqrt{1 - \alpha^2} + \sqrt{4 - \alpha^2}\,) \tag{C10}$$

are the positive roots in the γ_+ and γ_- cases, respectively.

Table I

Toroidal and Cylindrical Models Compared to Known Designs

	N&C	TOR	CYL	SPDE	TOR	CYL	RSSE	TOR	CYL
Results									
M_{core}/P_r	0.97	0.38	0.48	1.31	0.60	0.73	1.20	0.63	0.71
M_{coil}/P_r	0.39	0.41	0.29	0.90	0.59	0.41	0.41	0.62	0.40
M_m/P_r	0.30	0.29	0.21	0.27	0.31	0.21	0.33	0.42	0.31
M_c/P_r	N/A	→	→		0.14	0.14	0.15	0.17	0.18
M_{core}/M_{coil}	2.50	0.93	1.64	1.46	1.03	1.79	2.93	1.02	1.77
M_s/P_r	1.35	0.80	0.77	2.21	1.19	1.14	1.61	1.25	1.10
$(M_s+M_m)/P_r$	1.66	1.09	0.98	2.48	1.50	1.35	1.94	1.67	1.41
β	$1/\sqrt{2}$	→	→	2.22	0.45	0.47	1.49	0.57	0.59
Parameters									
α	$1/\sqrt{2}$	→	→	1.00	→	→	1.00	→	→
$P_r(/L)$	25	→	(26)	12.5	→	(15)	25	→	(28)
f	100	→	→	105	→	→	70	→	→
J_r	$5.0x10^6$	→	→	3.1E6	→	→	3.1E6	→	→
μ_{mr}	1.20	→	→	1.08	→	→	1.08	→	→
B_r	1.07	→	→	1.08	→	→	0.93	→	→
B_s	1.60	→	→	1.80	→	→	2.1	→	→
a_h	0.40	→	→	0.33	→	→	0.33	→	→
K_w	2.00	→	→	1.54	→	→	1.43	→	→
K_g	0.078	→	→	0.21	→	→	0.11	→	→
K_c	N/A	→	→		3.E-4	→		3.E-4	→

1. Specific masses are in units of kg/kW, P_r is in kW, P_r/L is in kW/m and is labeled by ( ), and all other units are MKS.
2. N&C is a design by Nasar and Chen[6], and SPDE and RSSE are designs by Mechanical Technology, Inc.[9,10].
3. TOR => Toroidal Model, CYL => Cylindrical Model.
4. N/A => not applicable. Blank space => value unknown. Some values for N&C, SPDE and RSSE are best estimates only.

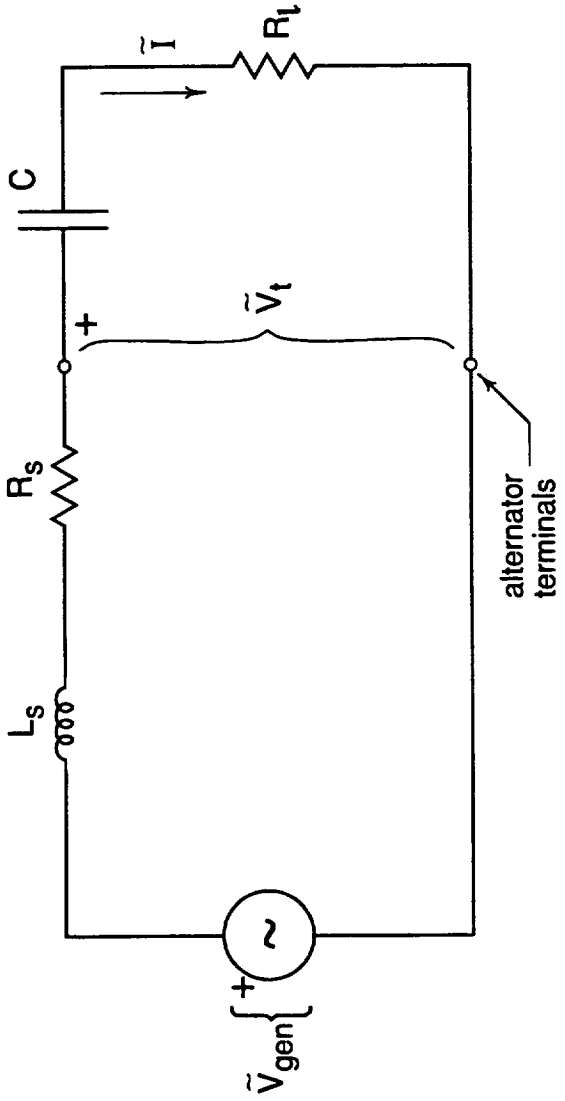

Figure 1. Elementary equivalent circuit of a resistively loaded and series capacitively tuned alternator.

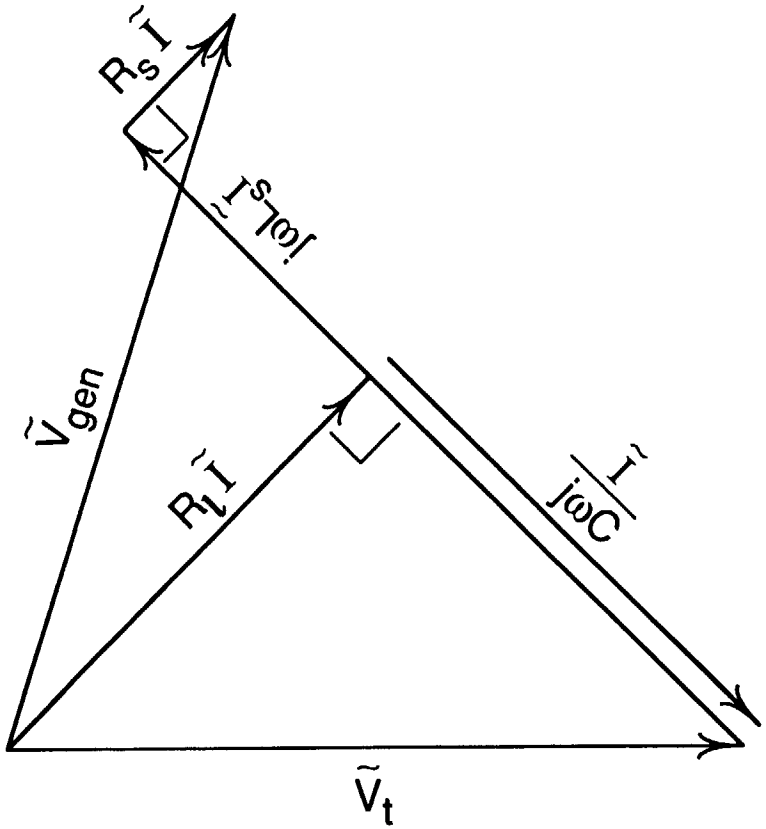

Figure 2. Voltage vector diagram for the equivalent circuit in Figure 1. Normally $R_s \ll R_l$.

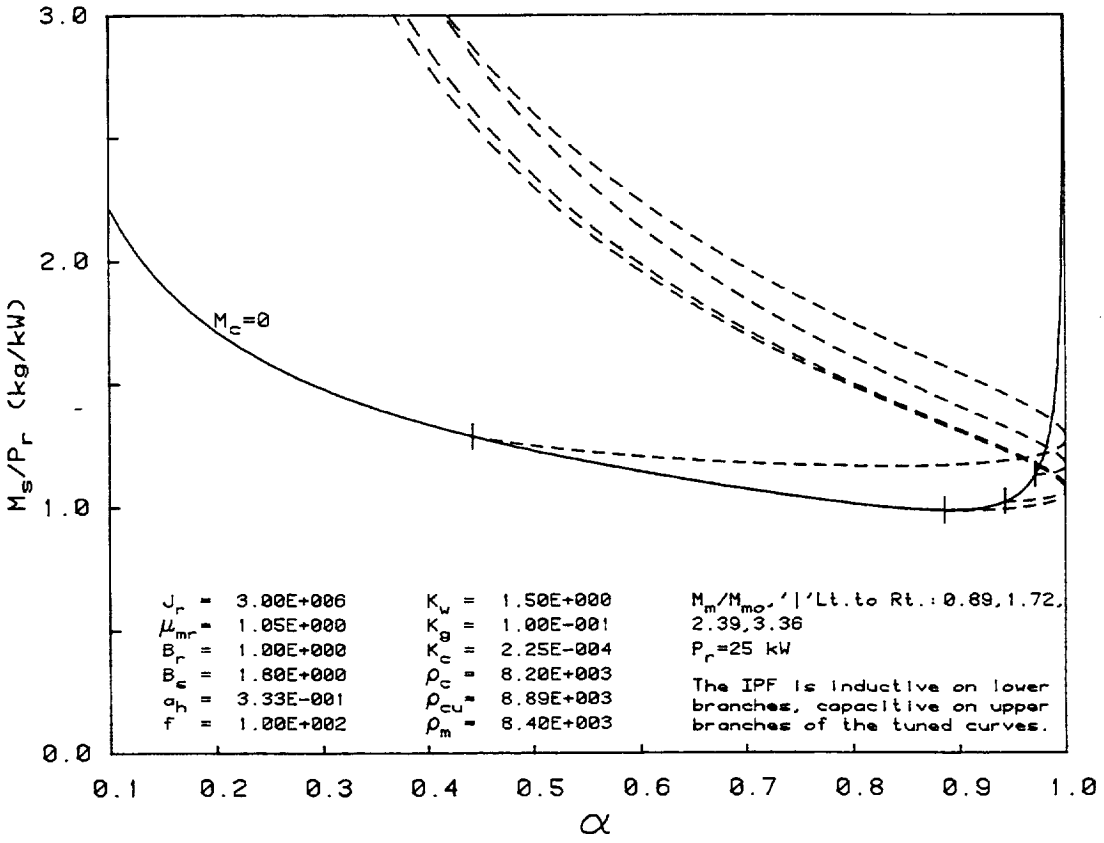

(A) Toroidal model.

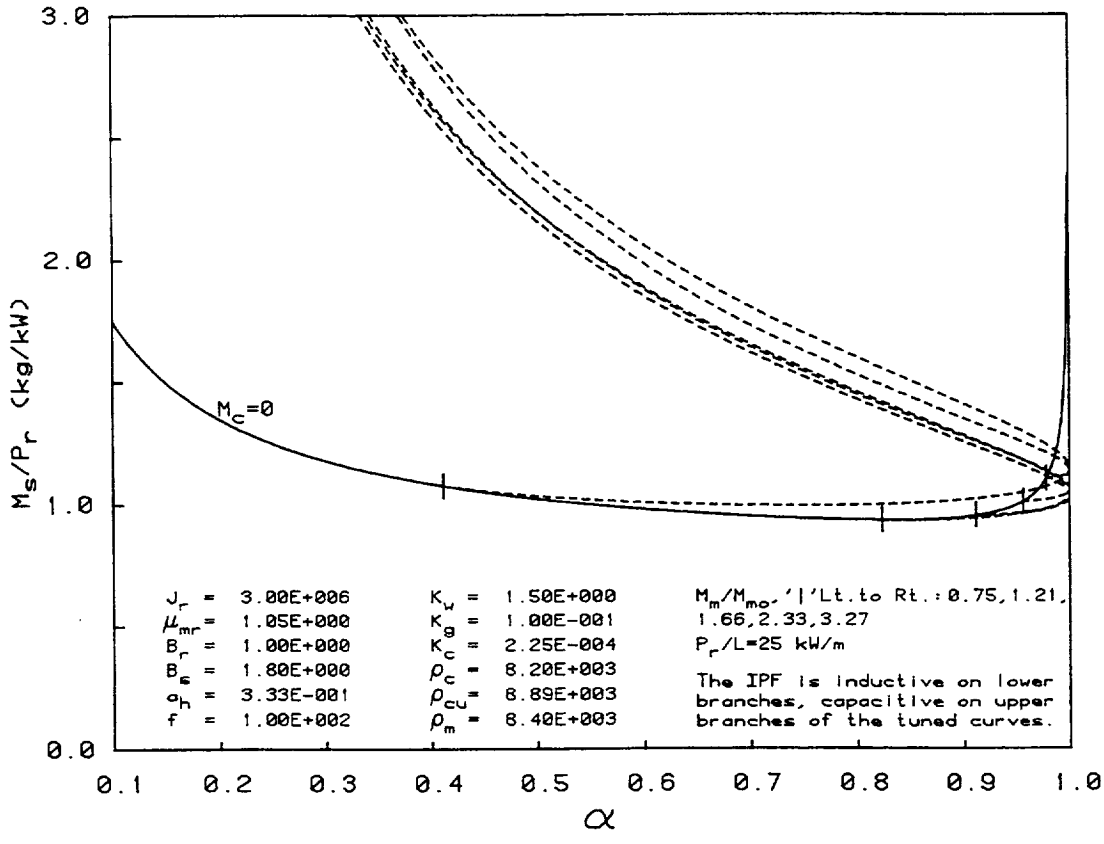

(B) Cylindrical model.

Figure 3. Plots of specific stator mass versus internal power factor with (dashed curves) and without (solid curve) capacitors. The tuned curves are drawn for various constant values of M_m/M_{mo} and their $C \to \infty$ limit is marked by '|' on the M_c=0 curve. Two magnet pairs are used.

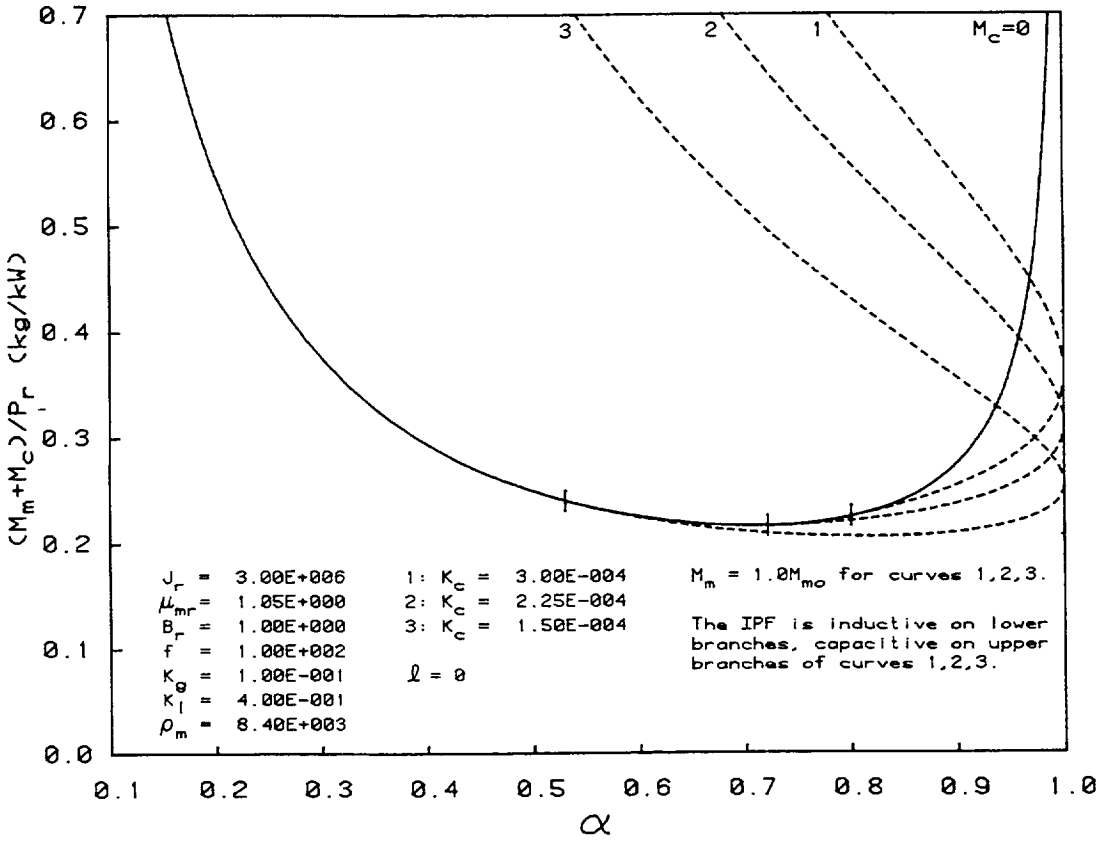

(A) M_m/M_{mo}=1, giving minimum $(M_m+M_c)/P_r$ in the tuned case.

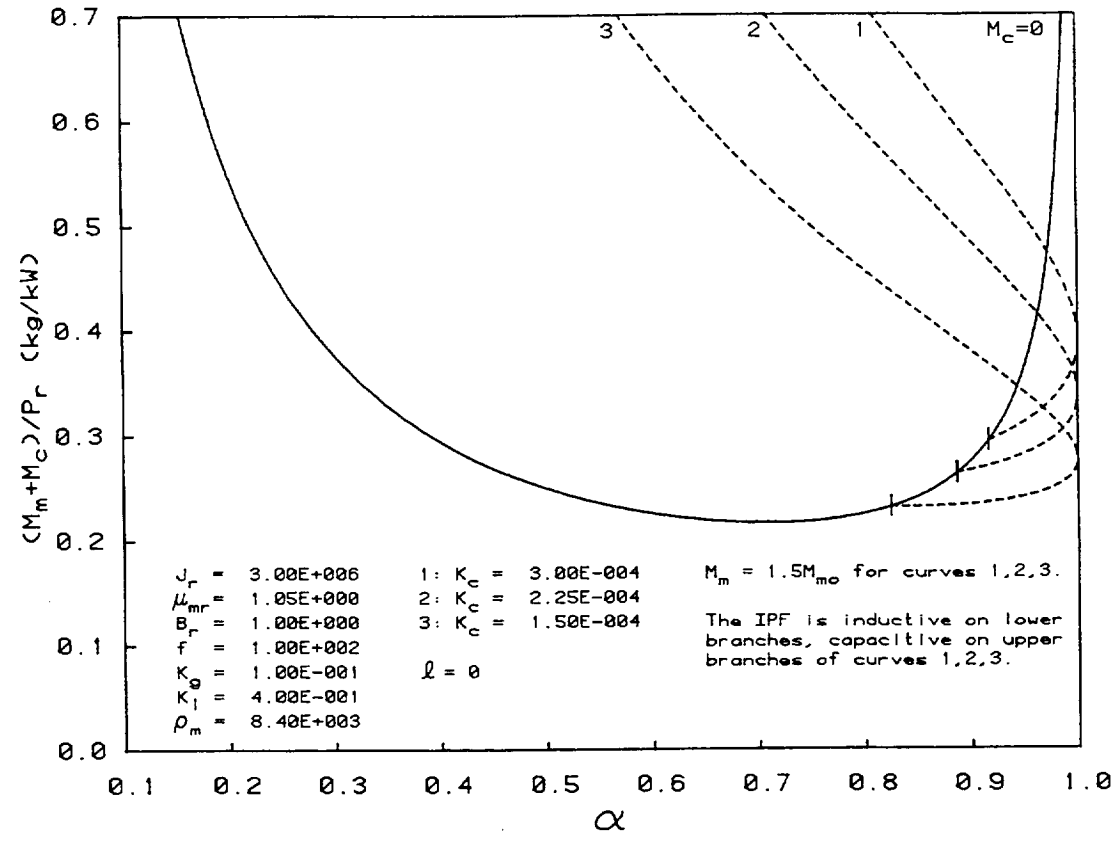

(B) M_m/M_{mo}=1.5, showing that this raises the tuned curves.

Figure 4. Plots of specific magnet plus capacitor mass versus internal power factor with (dashed curves) and without (solid curve) capacitors. The tuned curves are drawn for selected values of K_c and two choices of constant M_m/M_{mo}. The K_l used corresponds to $a_h \approx 1/3$ in the cylindrical model.

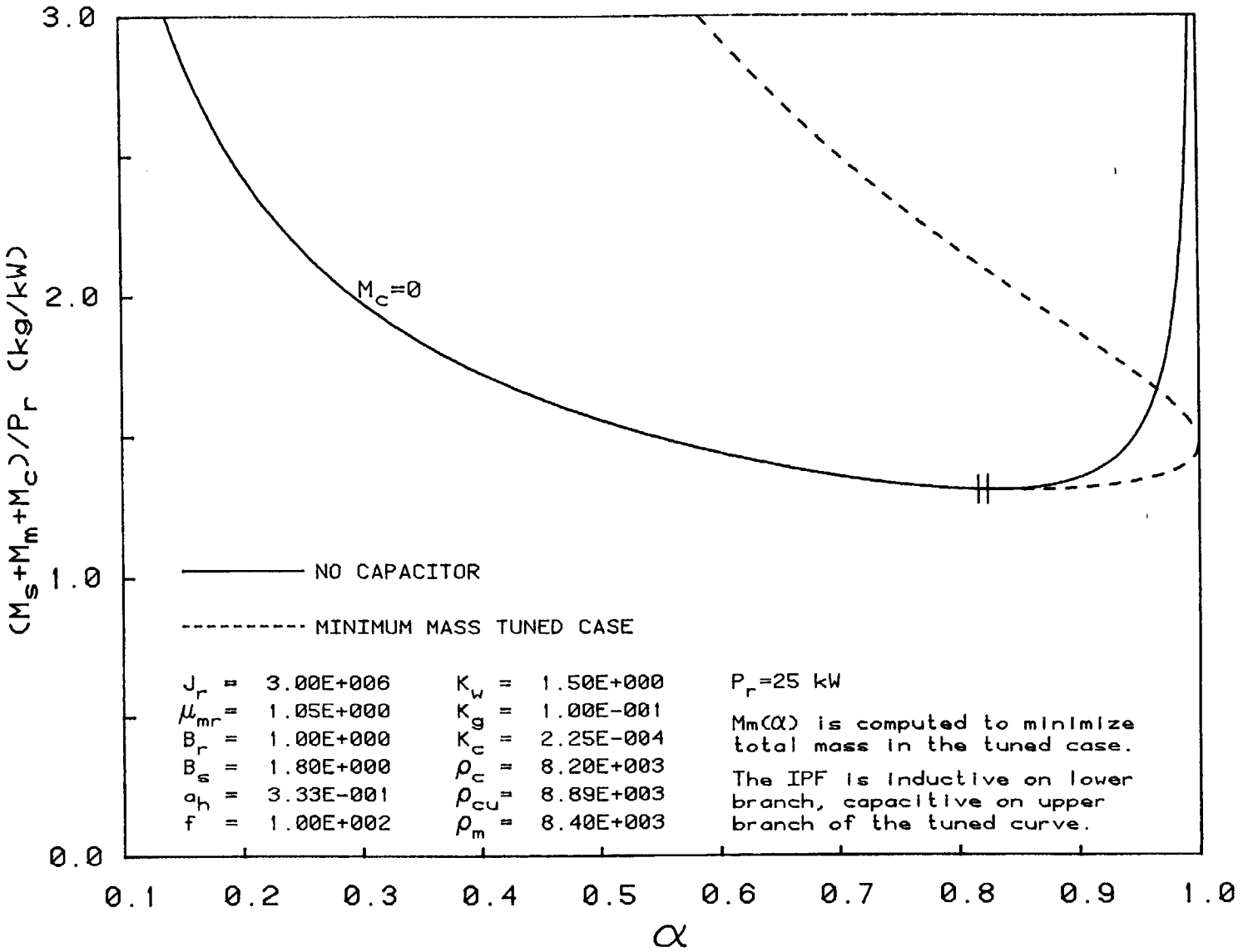

(A) Total specific mass versus internal power factor in the no-capacitor and mass-minimized tuned cases. Right '|' marks minimum on the nc curve and left '|' marks termination of the tuned inductive branch.

Figure 5. Specific mass composition of a minimum total mass tuned alternator compared to the no capacitor case, in the toroidal model.

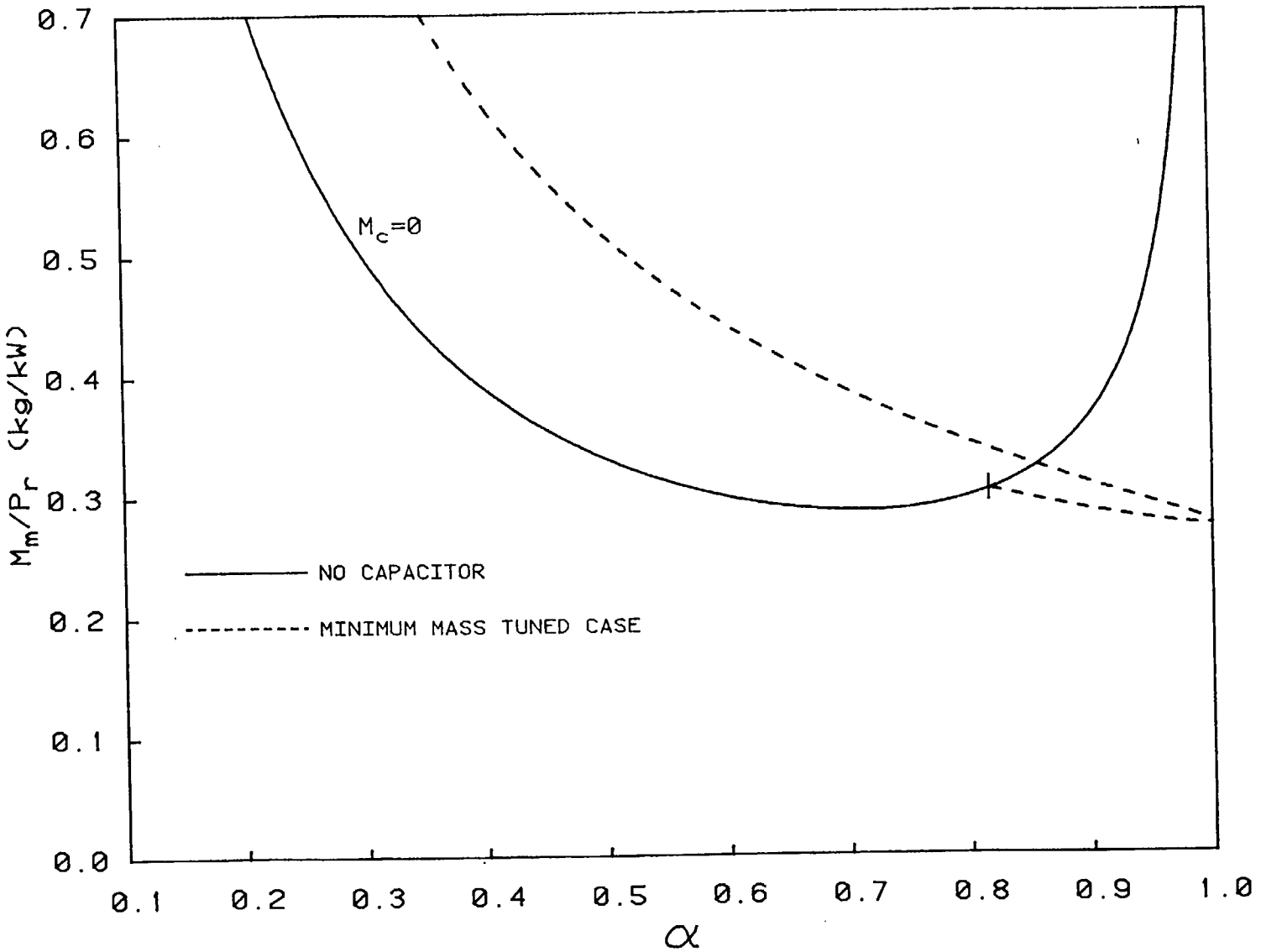

(B) Corresponding specific magnet mass versus internal power factor in the nc and mass-minimized tuned cases.

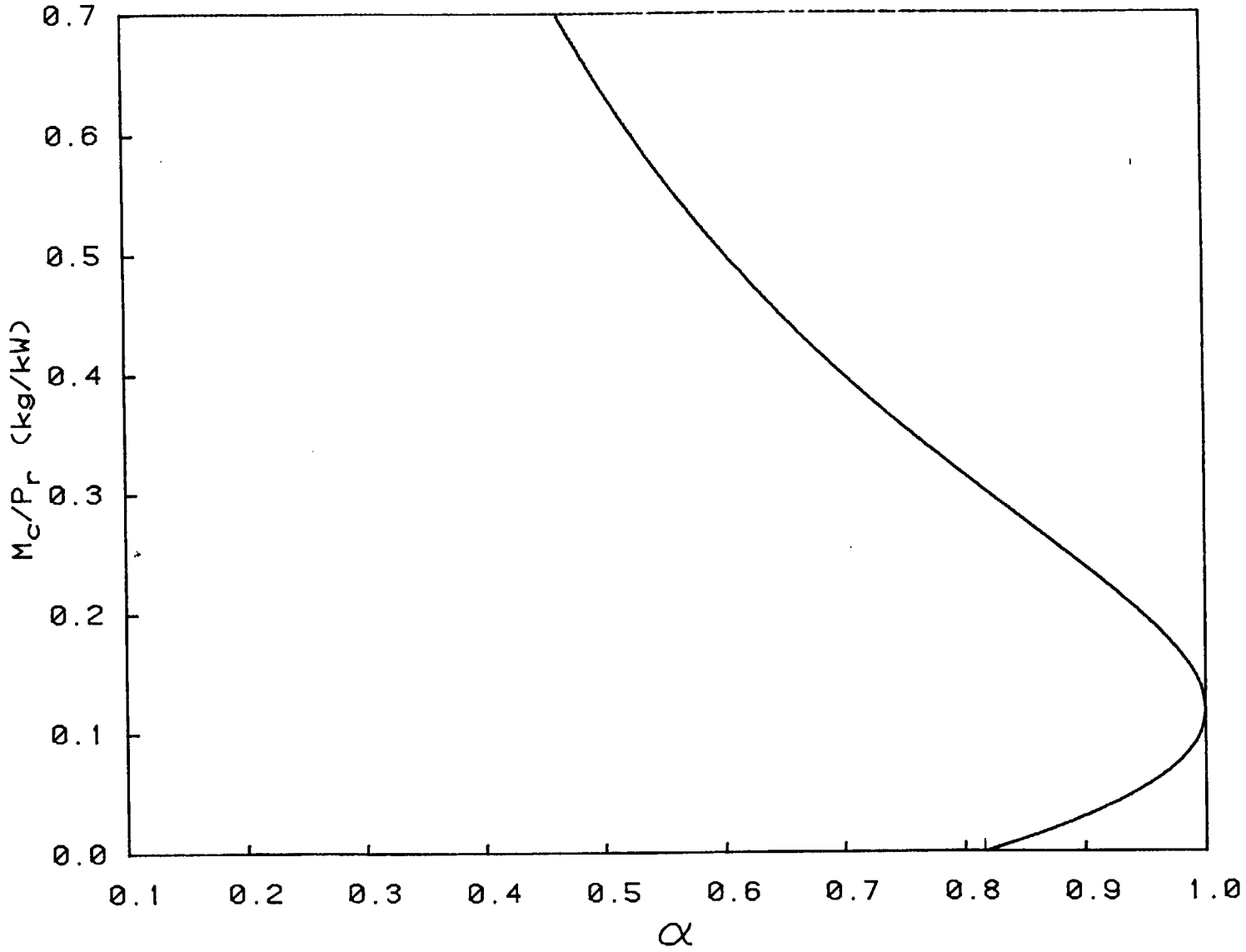

(C) Corresponding specific capacitor mass versus internal power factor in the mass-minimized tuned case.

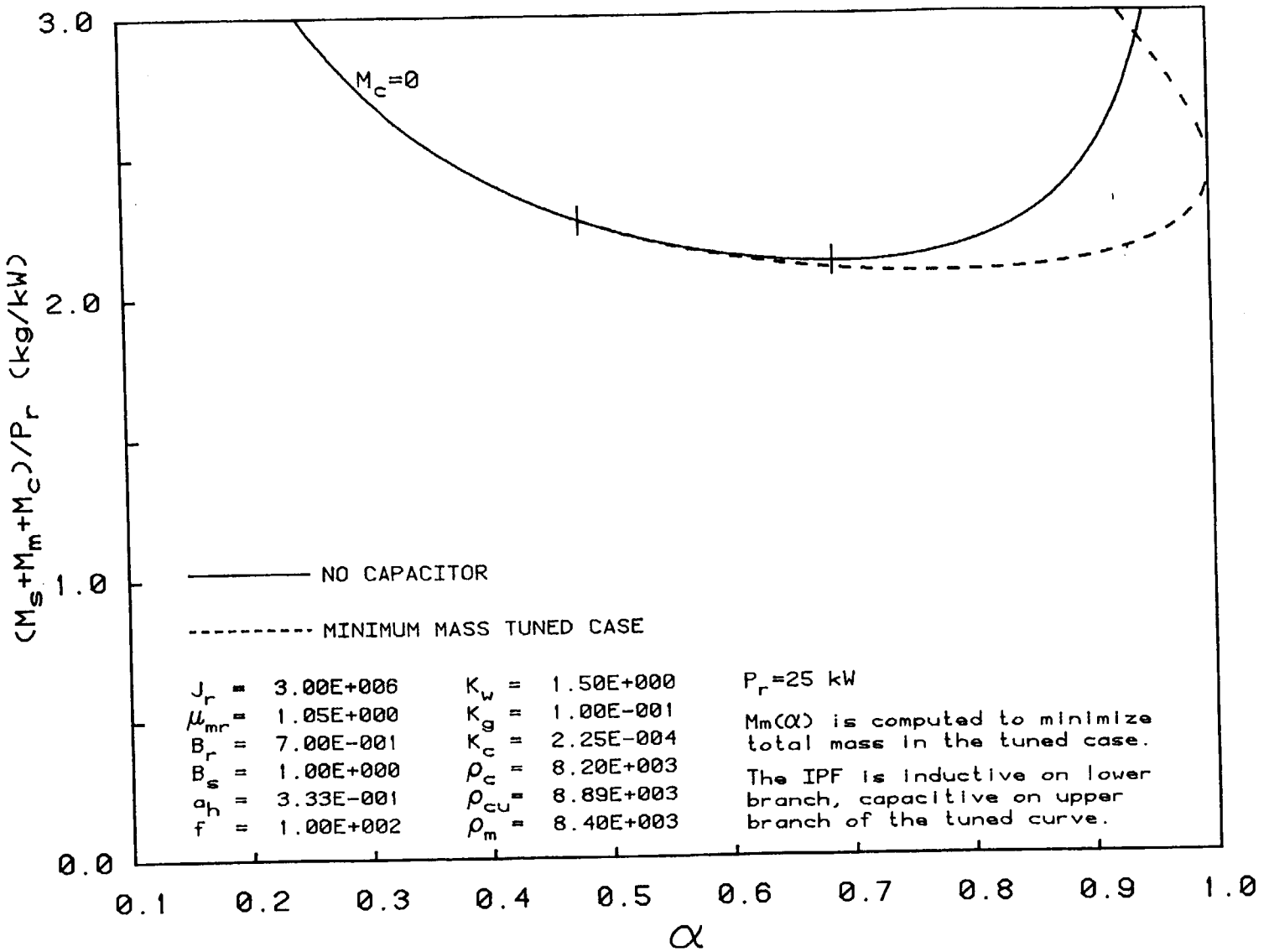

Figure 6. Increase in total specific mass in the no-capacitor and tuned cases due to reduced B_r and B_s (cf. Fig. 5A). Mass reduction available by tuning is also increased.

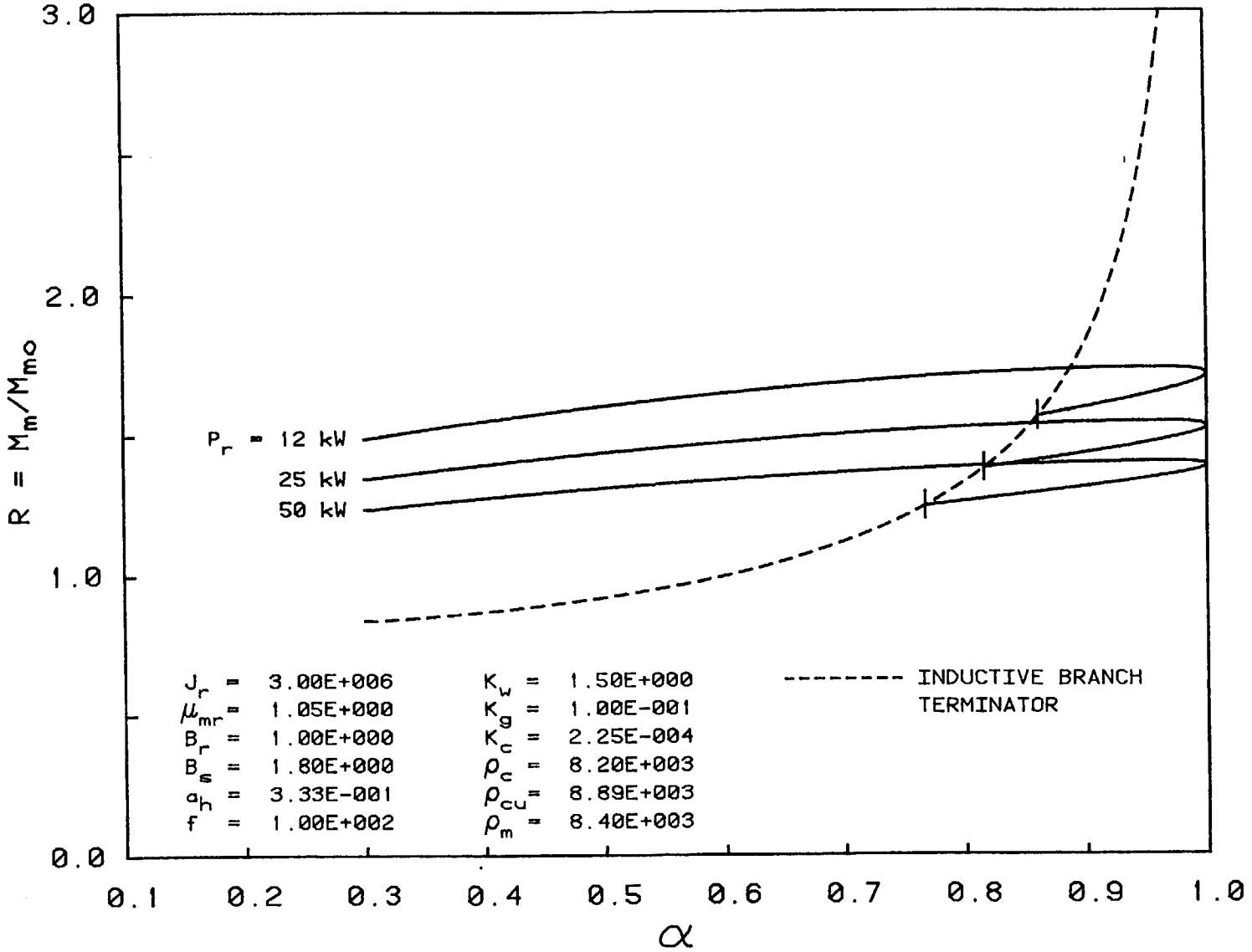

Figure 7. Normalized magnet mass versus internal power factor in the mass-minimized tuned toroidal model at selected power levels. The inductive branch terminator is the no-capacitor R.

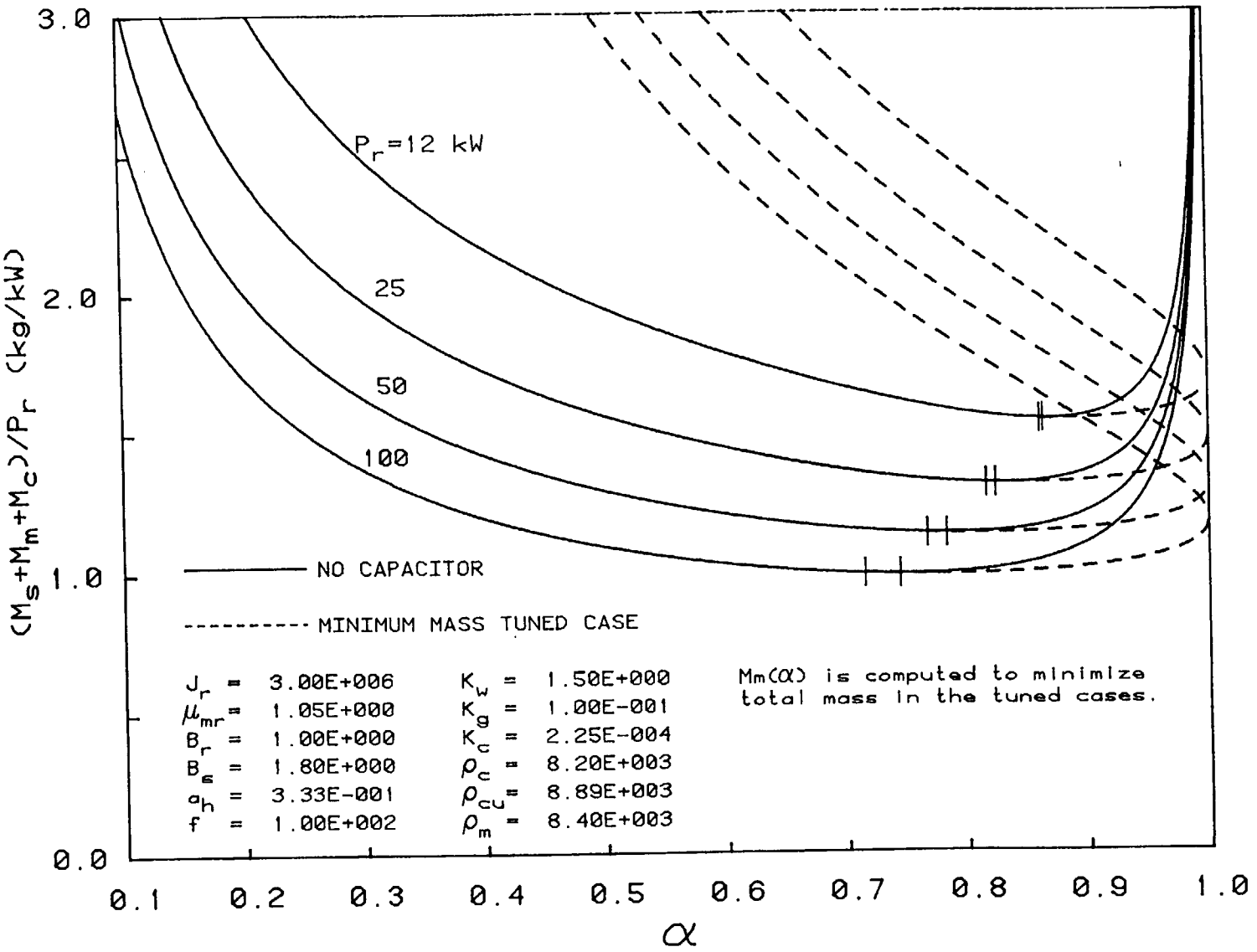

Figure 8. Load power scaling effect on the total specific mass in the toroidal model.

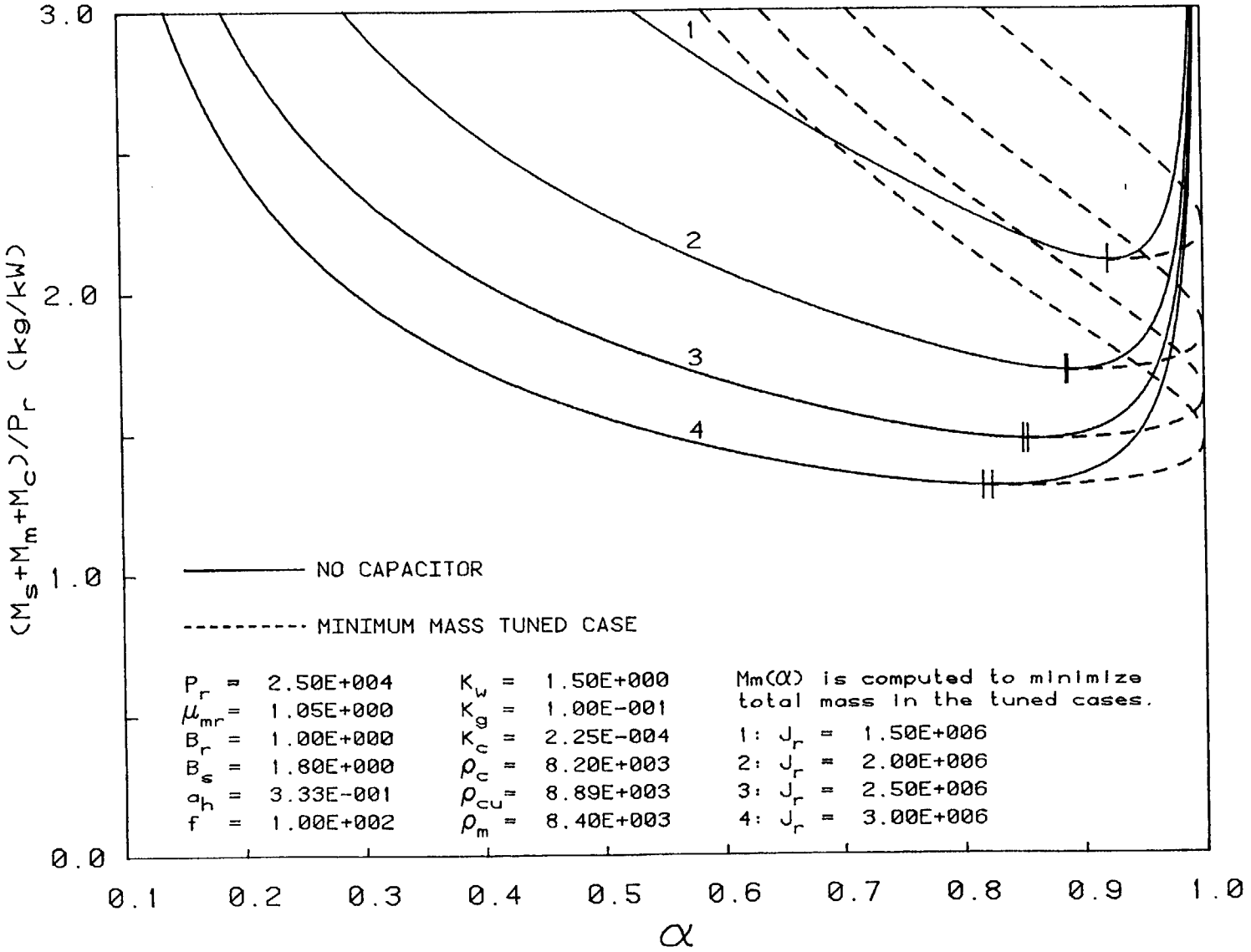

Figure 9. Current density scaling effect on the total specific mass in the toroidal model.

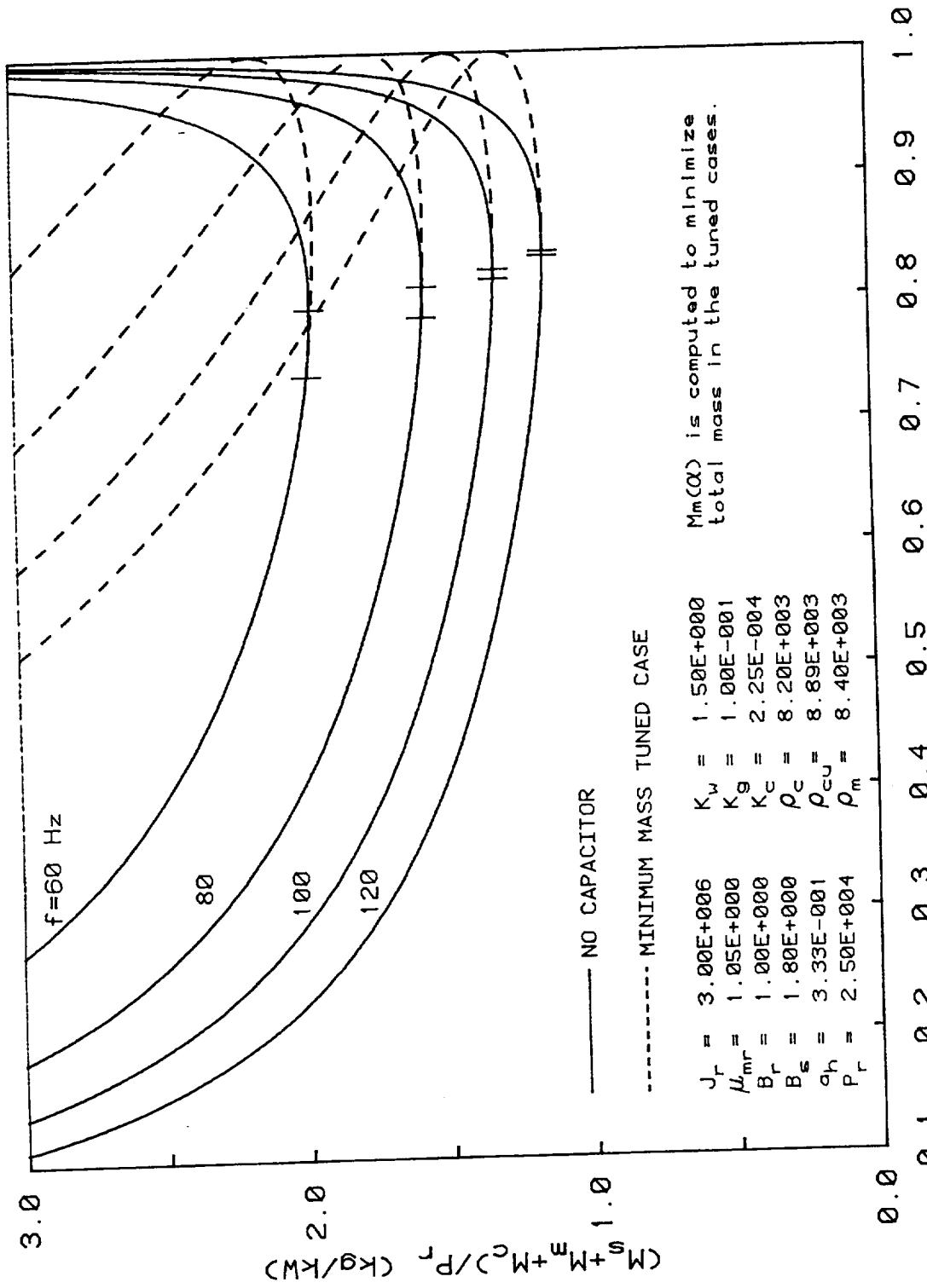

Figure 10. Frequency scaling effect on the total specific mass in the toroidal model.

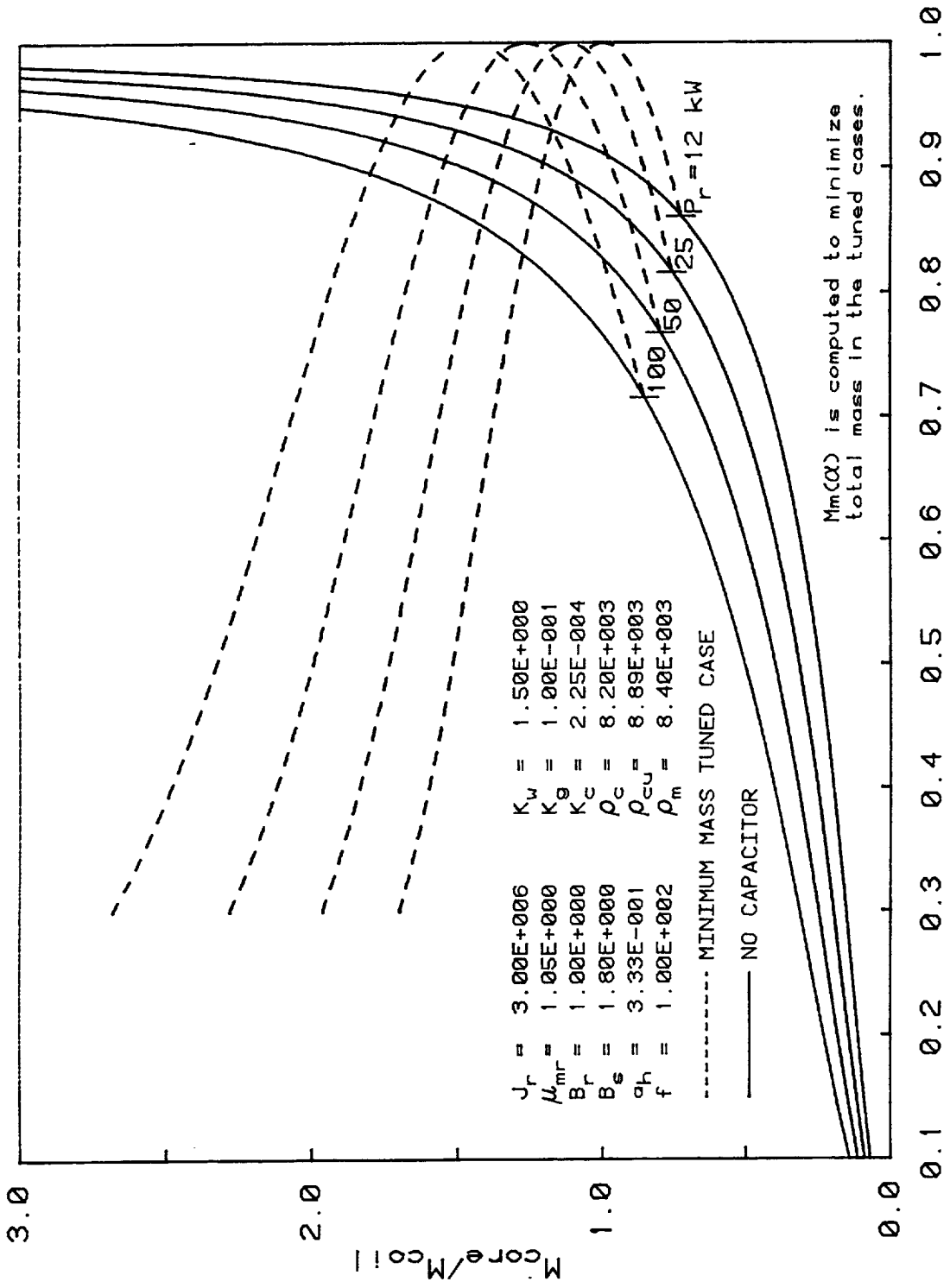

Figure 11. Load power scaling effect on the core-to-coil mass ratio in the toroidal model.

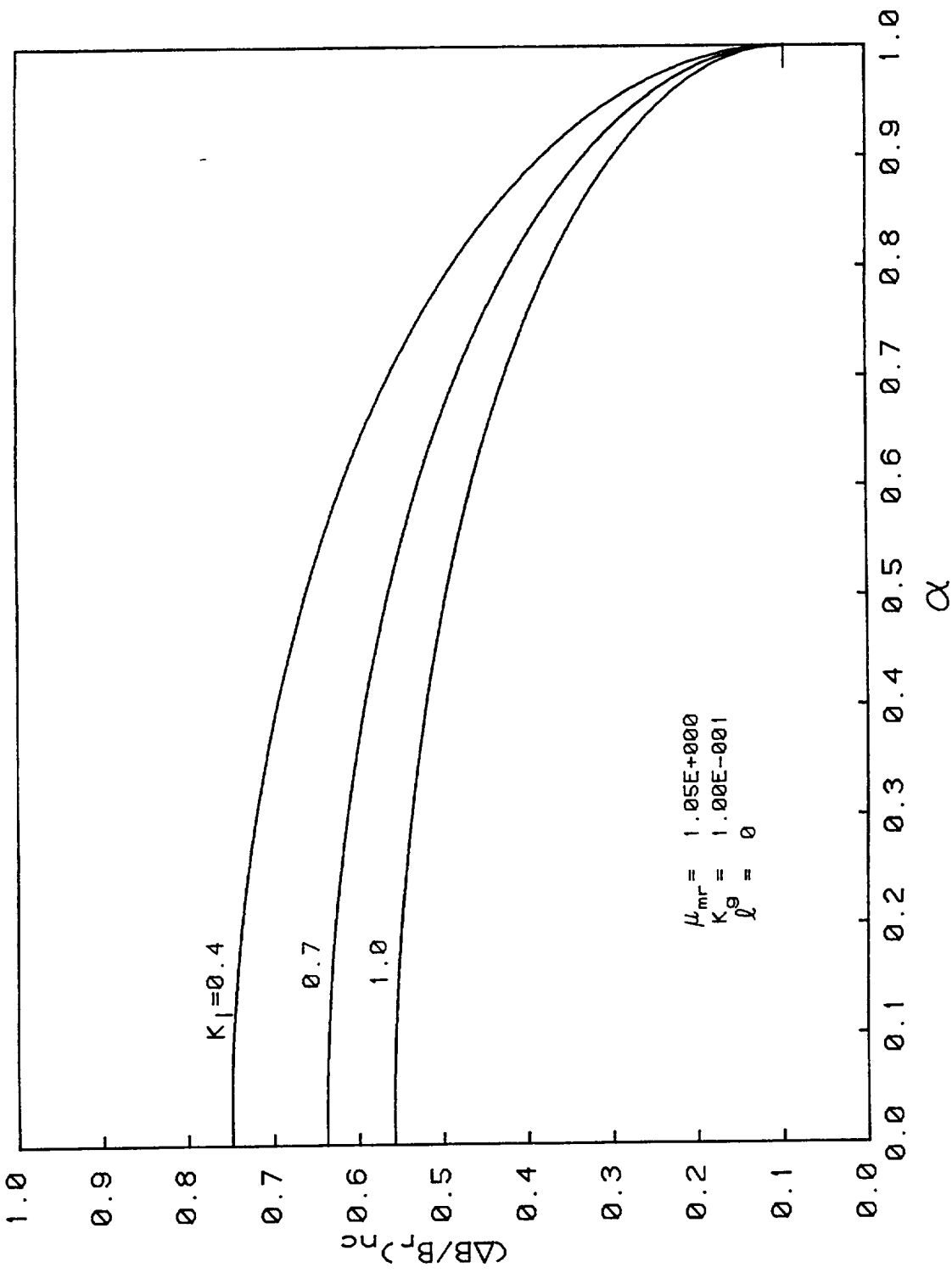

Figure 12. Normalized magnet reaction versus internal power factor in the no-capacitor case for selected gap flux fringing ratios K_l.

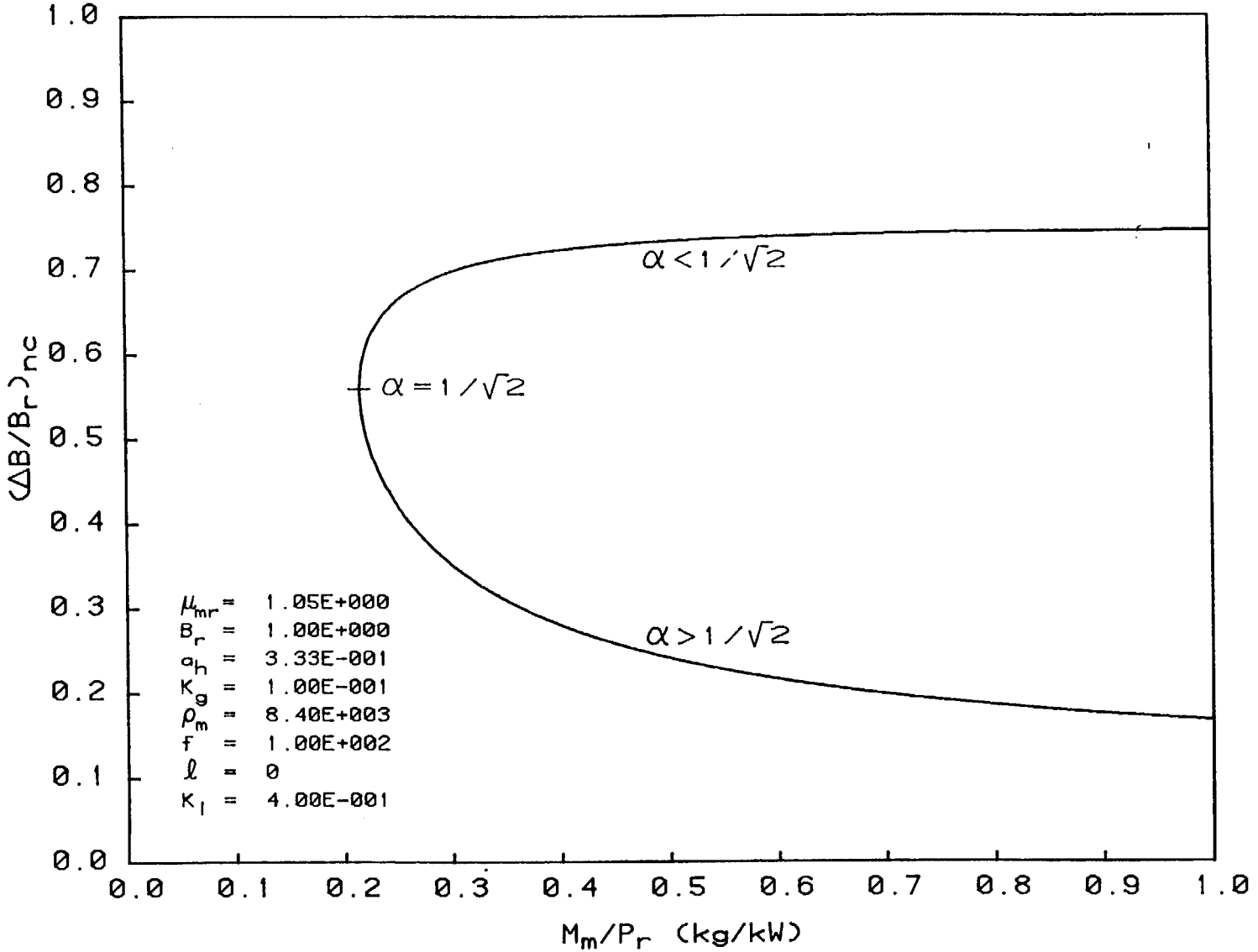

Figure 13. Normalized magnet reaction versus specific magnet mass for a selected gap flux fringing ratio K_ℓ.

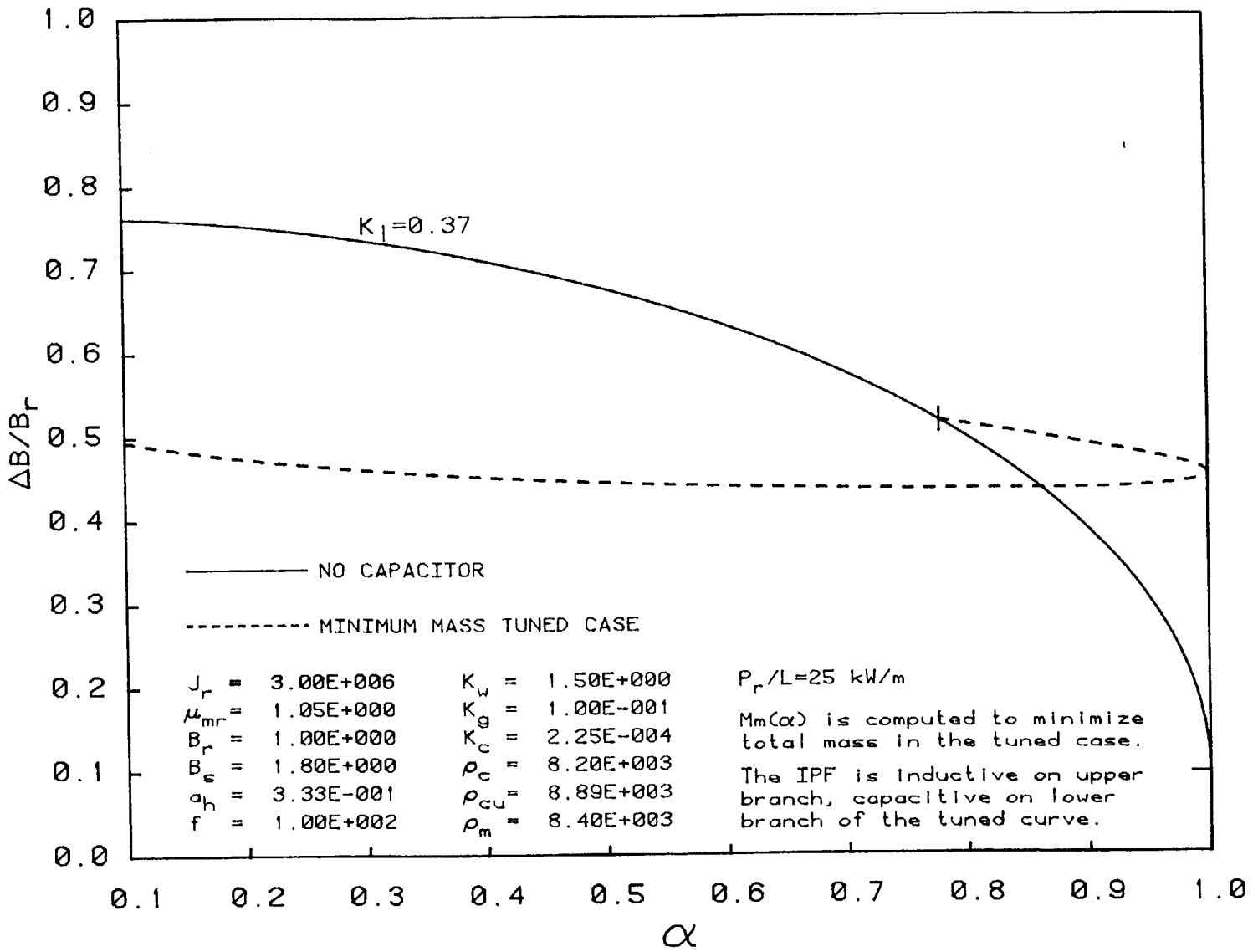

Figure 14. Normalized magnet reaction of a minimum mass, tuned cylindrical model compared to that of a no-capacitor design having the same gap flux fringing ratio. K_ℓ is computed by Eq. A19.

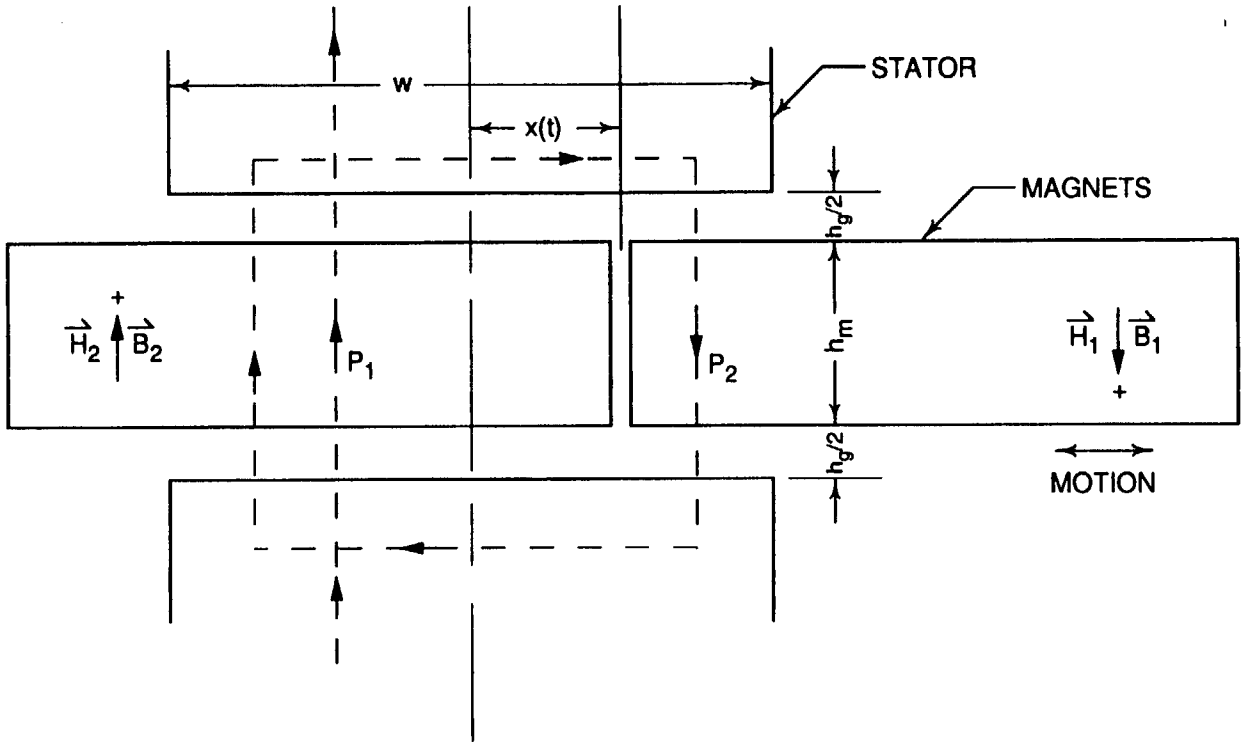

Figure A1. A pair of magnets moving together between stator pole faces. Integration paths P_1 and P_2 are shown dashed.

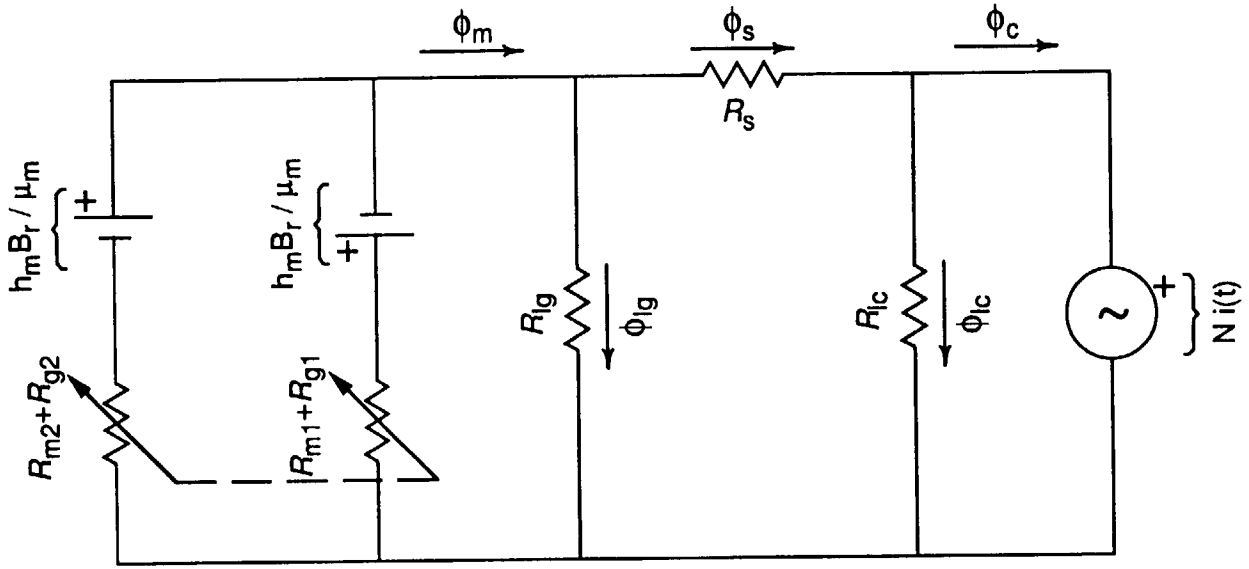

Figure A2. Equivalent magnetic circuit. The two constant magnet potential sources, each in series with a time-varying reluctance, are equvalent to a single time-varying source $(h_m B_r / \mu_m)\cdot(2\ x(t) / w)$ in series with the constant reluctance R_m+R_g.

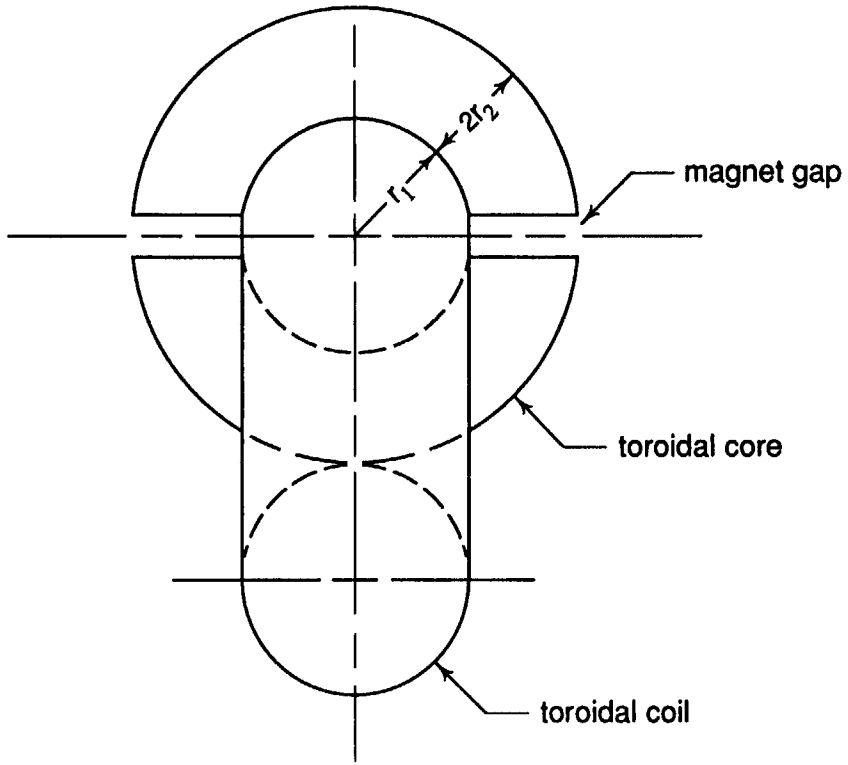

Figure B1. Core and coil shapes in a compactly linked toroidal geometry. Mechanically coupled magnet pairs may be thought to move in the gaps shown.

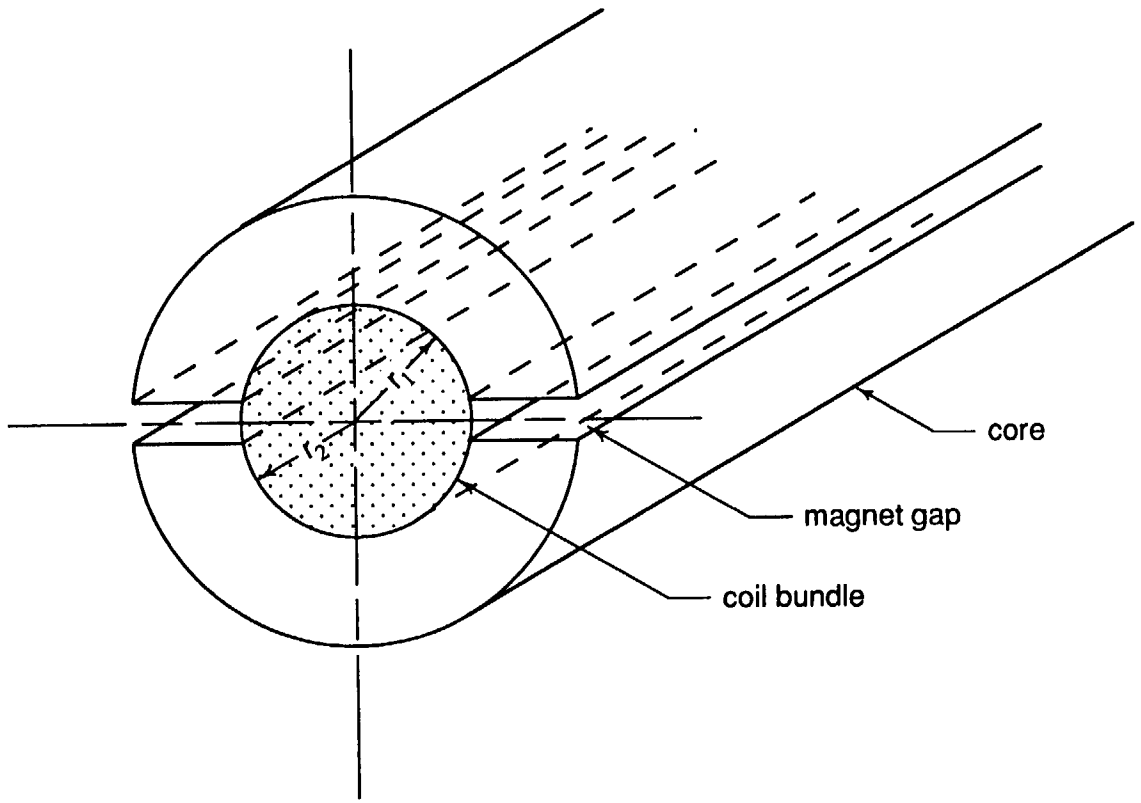

Figure B2. Core and coil shapes in a long cylindrical geometry. Magnetic flux encircles the bundle of parallel wires which fills the bore of the core. This geometry is to be thought of as curving around, closing the coil on itself. The magnet pairs in each gap are long, parallel strips, forming rings when the coil is closed.

REPORT DOCUMENTATION PAGE

Form Approved
OMB No. 0704-0188

1. AGENCY USE ONLY (*Leave blank*)	2. REPORT DATE	3. REPORT TYPE AND DATES COVERED
	June 1993	Final Contractor Report

4. TITLE AND SUBTITLE

Lightweight Linear Alternators With and Without Capacitive Tuning

5. FUNDING NUMBERS

WU–583–02–21
C–NAS3–25266

6. AUTHOR(S)

Janis M. Niedra

7. PERFORMING ORGANIZATION NAME(S) AND ADDRESS(ES)

Sverdrup Technology, Inc.
Lewis Research Center Group
2001 Aerospace Parkway
Brook Park, Ohio 44142

8. PERFORMING ORGANIZATION REPORT NUMBER

E–7929

9. SPONSORING/MONITORING AGENCY NAME(S) AND ADDRESS(ES)

National Aeronautics and Space Administration
Lewis Research Center
Cleveland, Ohio 44135–3191

10. SPONSORING/MONITORING AGENCY REPORT NUMBER

NASA CR–185273

11. SUPPLEMENTARY NOTES

Project Manager, Gene E. Schwarze, Power Technology Division, NASA Lewis Research Center, (216) 433–6117.

12a. DISTRIBUTION/AVAILABILITY STATEMENT

Unclassified - Unlimited
Subject Category 33

12b. DISTRIBUTION CODE

13. ABSTRACT (*Maximum 200 words*)

Permanent magnet excited linear alternators rated tens of kW and coupled to free-piston Stirling engines are presently viewed as promising candidates for long term generation of electric power in both space and terrestrial applications. Series capacitive cancellation of the internal inductive reactance of such alternators has been considered a viable way to both increase power extraction and to suppress unstable modes of the thermodynamic oscillation. Idealized toroidal and cylindrical alternator geometries are used here for a comparative study of the issues of specific mass and capacitive tuning, subject to stability criteria. The analysis shows that the stator mass of an alternator designed to be capacitively tuned is always greater than the minimum achievable stator mass of an alternator designed with no capacitors, assuming equal utilization of materials ratings and the same frequency and power to a resistive load. This conclusion is not substantially altered when the usually lesser masses of the magnets and of any capacitors are added. Within the reported stability requirements and under circumstances of normal materials ratings, this study finds no clear advantage to capacitive tuning. Comparative plots of the various constituent masses are presented versus the internal power factor taken as a design degree of freedom. The explicit formulas developed for stator core, coil, capacitor and magnet masses and for the degree of magnet utilization provide useful estimates of scaling effects.

14. SUBJECT TERMS

Linear alternator; Alternator mass; Alternator analysis; Power conversion; Permanent magnets; Stirling engine

15. NUMBER OF PAGES

57

16. PRICE CODE

A04

17. SECURITY CLASSIFICATION OF REPORT	18. SECURITY CLASSIFICATION OF THIS PAGE	19. SECURITY CLASSIFICATION OF ABSTRACT	20. LIMITATION OF ABSTRACT
Unclassified	Unclassified	Unclassified	